

# Dynamics and RG evolution of BH binaries via EFTs

BAPTS, October 2014  
Walter Goldberger  
Yale U.

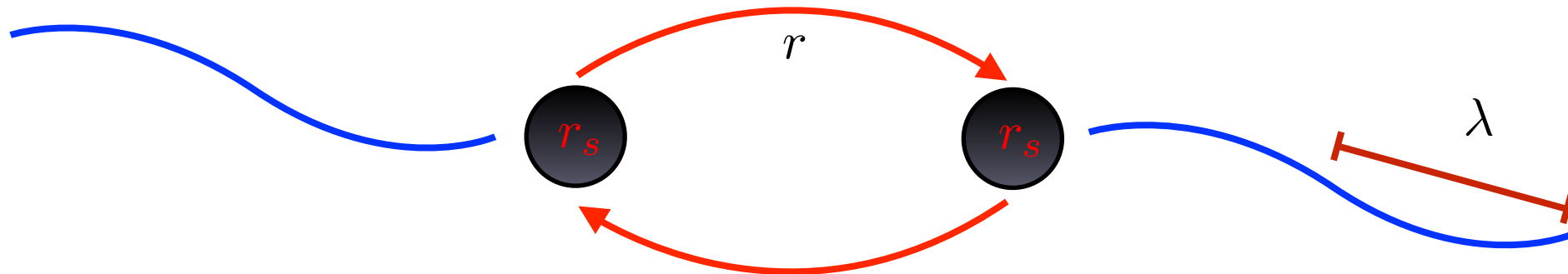
Based on: W.G., A. Ross, I. Rothstein ; PRD '13

⋮

W.G. + Rothstein, '04.

# Motivation:

Gravitational dynamics of radiating classical BH (or NS) binary systems in the non-relativistic limit are **experimentally relevant** (LIGO/VIRGO, LISA,...)



Even for  $v \ll 1$ , the non-linear nature of GR makes this a difficult problem, involving a hierarchy of length scales

Gravitational radius:	$r_g = 2G_N M$	$r_g \sim r_s \gg r \gg \lambda$
Physical radius:	$r_s (= r_g \text{ for BH})$	
Orbital scale:	$r$	
Radiation wavelength	$\lambda$	

Experiments will be sensitive to **at least**  $v^6$  corrections beyond Newtonian gravity (Thorne et al 1994). Numerical GR results also motivate computing higher order corrections.

In the NR limit  $v/c \ll 1$  these scales are correlated:

$$r \sim r_g/v^2$$

$$\lambda \sim r/v \sim r_g/v^3$$

Thus at a fixed order in velocity (“Post-Newtonian expansion”), physics effects from all these scales may appear.

This motivates an EFT formulation of the binary inspiral problem (WG+I. Rothstein, 2004).

Why EFT?

- Separation of scales

- Manifest power counting in expansion parameter.

- Systematic treatment of UV/IR divergences.

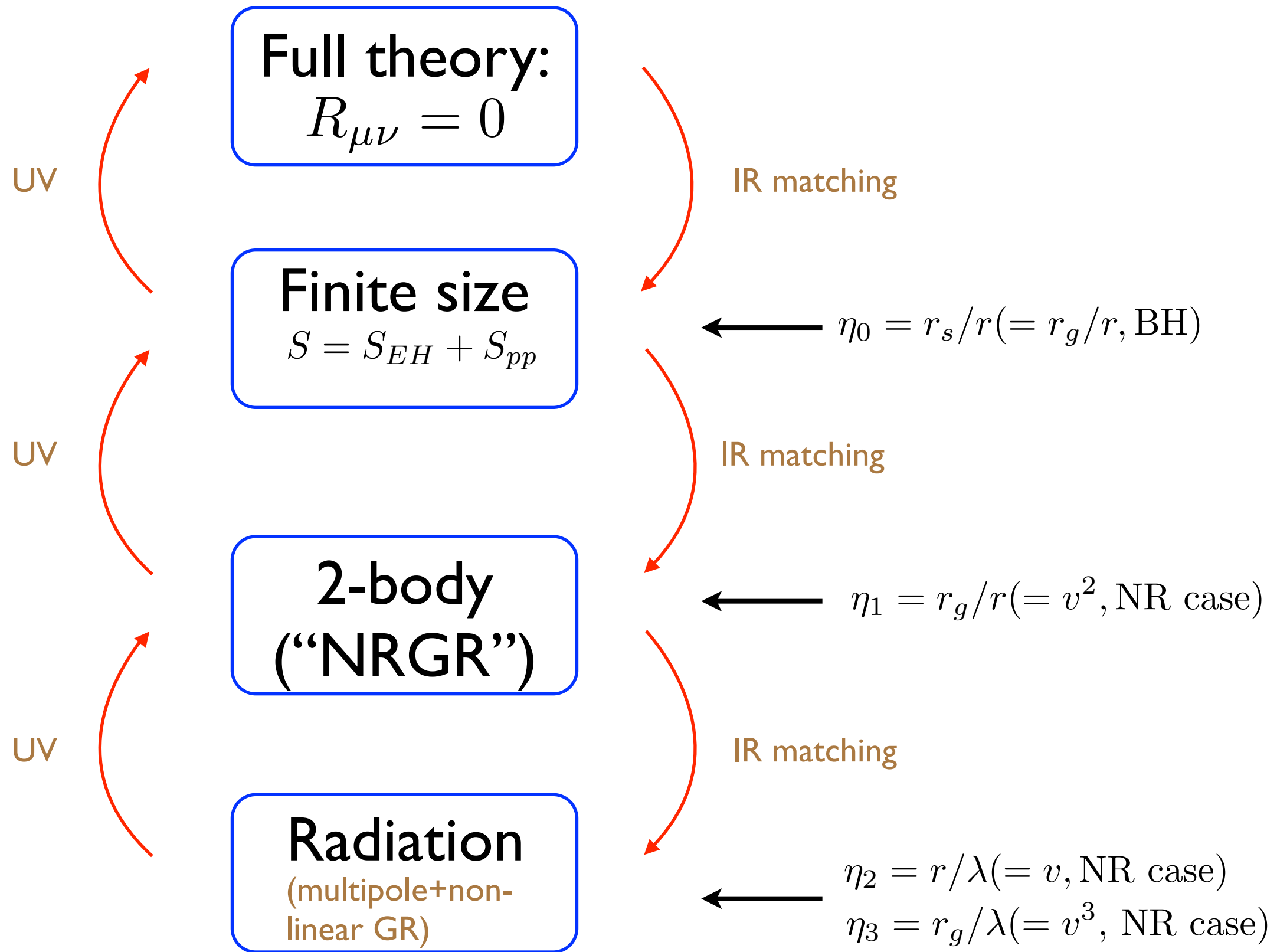
- Model independence by including all Lagrangian terms consistent with symmetries (in GR, diff. invariance).

- Resummation of non-analytic terms via the RG.

- ...

The correct set of EFTs for the binary system has properties in common w/ its gauge theory counterparts (HQET, NRQED/NRQCD,...)

# Tower of gravity EFTs:



Independent EFTs with distinct expansion parameter coincide in PN limit.

UV divergence in  $\text{EFT}_{i+1}$  corresponds to IR effect in  $\text{EFT}_i$

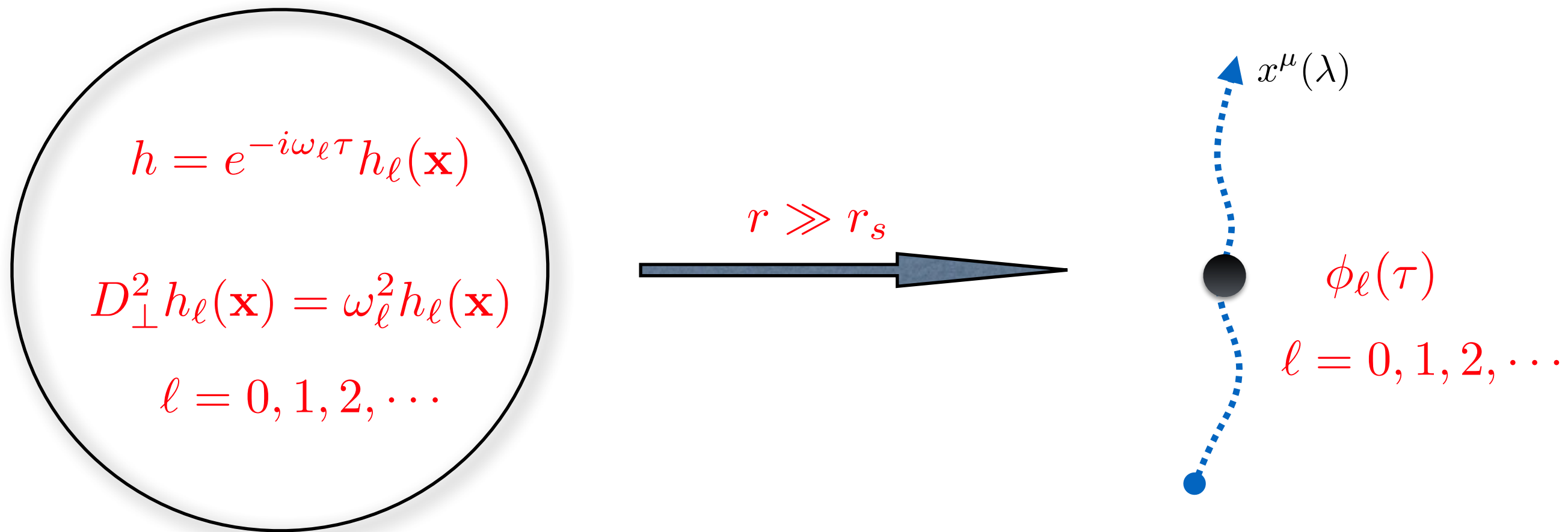


# The EFTs:

At each stage in the calculation, the relevant modes are worldline localized (0+1) dim d.o.f's with local  $SO(3)$  indices, coupled to gravity.

Consider first isolated BH/NS. Then these dynamical moments are just the normal (or “quasi-normal”) modes of the field theory (matter+gravitational) that makes up the compact star.

Heuristically, matching onto the worldline EFT is just dimensional reduction:



eg, for a Schwarzschild black hole, the spectrum contains an infinite tower of modes. In this case there are some zero modes:

Mode	Freq.	$J^P$
$m(\lambda)$	0	0
$x^\mu(\lambda)$	0	$1^+$
$\omega_{ij}(\lambda)$ (spin)	0	$1^-$

there are also massive “states”:

n	$\ell = 2$		$\ell = 3$		$\ell = 4$	
0	0.37367	-0.08896 i	0.59944	-0.09270 i	0.80918	-0.09416 i
1	0.34671	-0.27391 i	0.58264	-0.28130 i	0.79663	-0.28443 i
2	0.30105	-0.47828 i	0.55168	-0.47909 i	0.77271	-0.47991 i
3	0.25150	-0.70514 i	0.51196	-0.69034 i	0.73984	-0.68392 i

Table 1: *The first four QNM frequencies ( $\omega M$ ) of the Schwarzschild black hole for  $\ell = 2, 3$ , and 4 [135]. The frequencies are given in geometrical units and for conversion into kHz one should multiply by  $2\pi(5142Hz) \times (M_\odot/M)$ .*

(from Kokkotas and Schmidt, gr-qc/9909058).

Effective Lagrangian is built from these modes and the gravitational field  $g_{\mu\nu}(x)$

At long distances, EFT of worldline localized modes coupled to curvature:

$$S = S_{EH} + S_{pp}$$

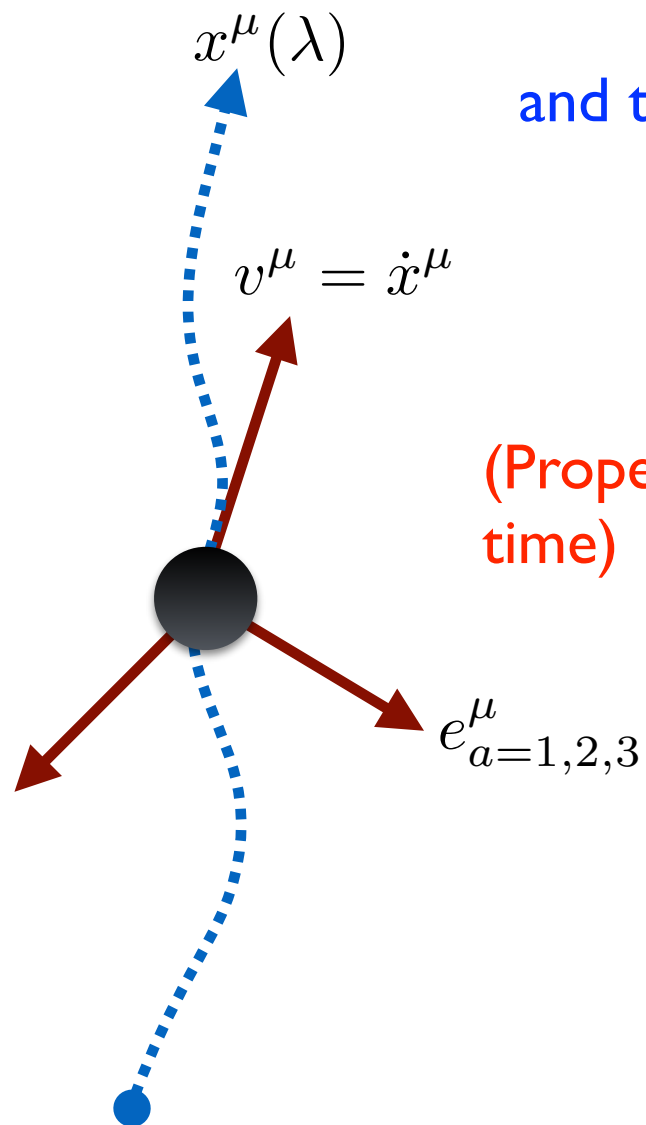
w/  $S_{EH} = -2m_{Pl}^2 \int d^4x \sqrt{g} R(x)$  ( $\hbar = c = 1$ )  
( $m_{Pl}^2 = 1/(32\pi G_N)$ )

and the gravitational “Wilson line” action (WG+Rothstein, 2005)

$$S_{pp} = - \int d\tau(\lambda) m(\lambda) - \int dx^\mu L_{ab}(\lambda) \omega_\mu^{ab}(x(\tau))$$

$$+ \frac{1}{2} \int d\tau(\lambda) Q_E^{ab}(\lambda) E_{ab}(x(\lambda)) + \frac{1}{2} \int d\tau(\lambda) Q_B^{ab}(\lambda) B_{ab}(x(\lambda))$$

(Proper  
time)



BH spin=rotating frame  $e_{a=1,2,3}^\mu$  (see R. Porto gr-qc/0511061, and S. Endlich et al, arXiv:1405.7384) = non-linear realization  $SO(3,1)/SO(3)$

Dynamical  
mass mode=  $m(\lambda)$  (WG, Ross, Rothstein 2013)

Curvature in comoving frame:

$$E_{ab} = e_a^\alpha e_b^\beta v^\mu v^\nu R_{\mu\alpha\nu\beta} = \text{“electric Riemann tensor”}$$

$$B_{ab} = \frac{1}{2} e_a^\alpha e_b^\beta v^\mu v^\lambda \epsilon_{\alpha\mu\rho\sigma} R_\beta^{\lambda\rho\sigma} = \text{“magnetic Riemann tensor”}$$

For a Schwarzschild BH, the  $\ell \geq 2$  modes are “heavy,” w/  $r_s \omega_n \sim \mathcal{O}(1)$ . However, because

$$\text{Im } \omega_n \neq 0$$

integrating out the dynamical quadrupole  $Q_{ab}(\lambda)$  would result in a **non-local** worldline effective action. We have no choice but to keep them and the theory, and relate any observable quantity to the “response functions”

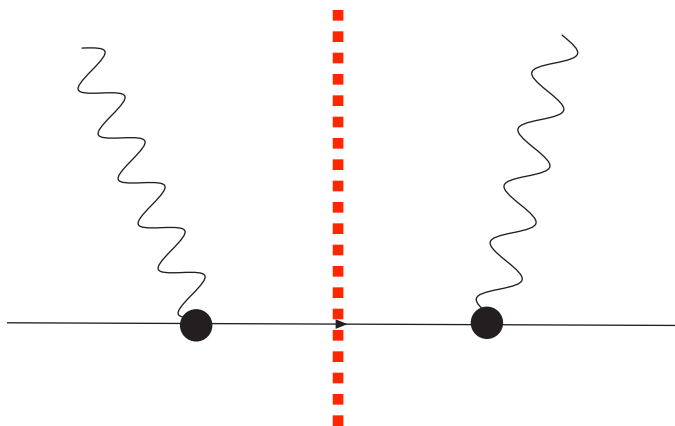
$$\langle Q^{E,B} \dots Q^{E,B} \rangle$$

Classically we only need to keep the two-pt. function. In the rest frame of a (non-spinning) BH:

$$\int dx^0 e^{-i\omega x^0} \langle T Q_{ab}^E(0) Q_{cd}^E(x^0) \rangle = -\frac{i}{2} \left[ \delta_{ac} \delta_{bd} + \delta_{ad} \delta_{bc} - \frac{2}{3} \delta_{ab} \delta_{cd} \right] F(\omega),$$

(this is a classical object, related to the graviton propagator in the BH background). The imaginary part is related to the **graviton absorption cross section** (WG + Rothstein, 2005)

The function



$$\sigma_{abs,p}(\omega) = \frac{\omega^3}{2m_{Pl}^2} \text{Im} F(\omega).$$

Compare to the result in the full theory (Starobinsky; Page, 1970's):

$$\sigma_{abs,p}(\omega) = \frac{1}{45} 4\pi r_s^6 \omega^4,$$



$$\text{Im}F(\omega) = 16G_N^5 m^6 \omega / 45$$

This result can be used to predict energy dissipation by BH horizons in two-body bound state (WG+Rothstein, 2005)

$$\frac{dP_{abs}}{d\omega} = -\frac{1}{T} \frac{G_N}{64\pi^2} \sum_{a \neq b} \frac{\sigma_{abs}^{(b)}(\omega)}{\omega^2} m_a^2 |q_{ij}^{(a)}(\omega)|^2,$$

Time averaged rate of energy dissipation:

$$P_{abs} = \frac{32}{5} G_N^7 m^6 \mu^2 \left\langle \frac{\mathbf{v}^2}{|\mathbf{x}|^8} + 32 \frac{(\mathbf{x} \cdot \mathbf{v})^2}{|\mathbf{x}|^{10}} \right\rangle$$

The real part of the function encodes **tidal response** to an applied curvature field

$$\langle Q_{ab}(\omega) \rangle = -\frac{1}{2} F(\omega) E^{ab}(\omega) = \text{Induced quadrupole moment}$$

This was calculated by Steinhoff et al (2013) by comparing full BH and EFT:



$$\text{Re}F(\omega) = 0 + \mathcal{O}(\omega^2)$$

i.e no static tidal response for a 4d Schwarzschild BH!(?) (see also Kol+Smolkin, 2011 for  $d \neq 4$  ).

Note that because  $F(\omega) \sim G_N^5$ , finite size effects for a BH do not arise until “4 PN” ( $v^8$ ) order. To a good approx they are point objects. However, expect some enhancement for NS

$$r_{NS}/r_s \sim 10$$

although difficult to get model-independent results for response functions in this case.

# EFT II: 2-body bound state

This is a theory of 2 pt non-relativistic particles, interacting gravitationally and emitting radiation:

$$S = S_{EH} + S_{pp}$$

where now,

$$S_{pp} = - \sum_{a=1,2} \int d\tau_a m_a + \sum_{a=1,2} \int d\tau_a \left( c_a^E E_{\mu\nu}^2 + c_a^B B_{\mu\nu}^2 \right) + \dots$$

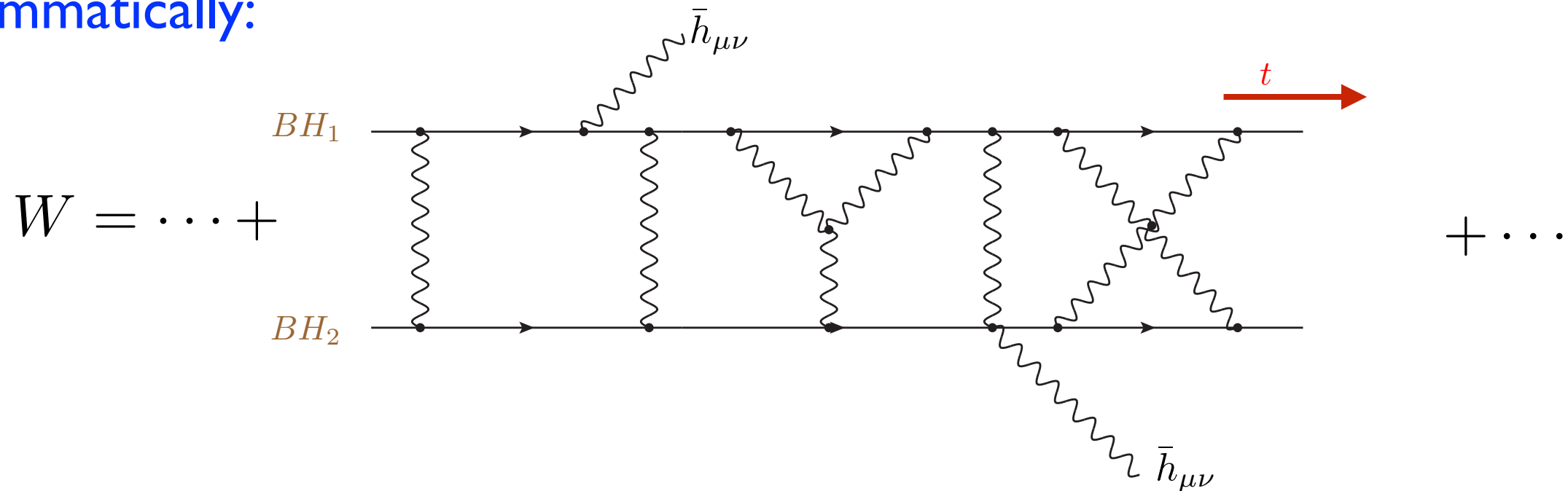
ignoring spin, finite size, etc.

# The gravitational “Wilson line”

$$W = \exp i\Gamma[\bar{h}, x_a] = \int [\mathcal{D}h_{\mu\nu}]_{\text{b.c.'s}} e^{iS[h, \bar{h}, x_a]}$$

generates all the observables of the (classical) binary system.

Diagrammatically:



$$= e^{\Sigma(\text{BH irreducible diagrams})}$$

where we split up the metric into a background field and a “fluctuating part”:

$$g_{\mu\nu} = \eta_{\mu\nu} + \bar{h}_{\mu\nu} + h_{\mu\nu}$$

background

fluctuation

and integrate out fluctuations.



For example,

$$\Gamma[\bar{h} = 0, x_a] = \int dt L(\mathbf{x}_a(t), \dot{\mathbf{x}}_a(t)) = \text{two-body Lagrangian}$$

generates the equations of motion for the BH trajectories

The linear term in the background defines an effective energy-momentum tensor:

$$\Gamma[\bar{h} =, x_a] = \cdots + \frac{1}{2m_{Pl}} \int d^4x T^{\mu\nu}(x) \bar{h}_{\mu\nu} + \cdots$$

$$\partial_\mu T^{\mu\nu}(x) = 0$$

(Ward id. for diff invariance)

which can be used to compute radiation at infinity

In particular, with standard in/out (Feynman) b.c.'s, graviton emission amplitude is

$$\mathcal{A}_{h=\pm 2}(k) = \int d^4x e^{ik \cdot x} \epsilon_{\mu\nu}^*(h, k) T^{\mu\nu}(x)$$

and the graviton emission rate over  $T \rightarrow \infty$

$$d\Gamma_h(\mathbf{k}) = \frac{1}{T} \frac{d^3\mathbf{k}}{(2\pi)^3 2|\mathbf{k}|} |\mathcal{A}_h(\mathbf{k})|^2,$$

yield time-averaged energy and momentum emission rates:

$$\langle \dot{P}^\mu \rangle_{h=\pm 2} = \int k^\mu d\Gamma_h(\mathbf{k}),$$

$$\langle \dot{\mathbf{J}} \rangle = 2 \int \mathbf{n} d\Gamma_{h=2}(\mathbf{k}) - 2 \int \mathbf{n} d\Gamma_{h=-2}(\mathbf{k}),$$

Using in/in boundary conditions (as in cosmology) gives instantaneous observables, e.g. radiation field at infinity:

$$h_{\mu\nu}(\mathbf{x} \rightarrow \infty, t) = \int d^4y D_{\mu\nu;\alpha\beta}^{\text{ret}}(x - y) T^{\alpha\beta}(y)$$

which yields the time-dep. waveform seen in the detector.

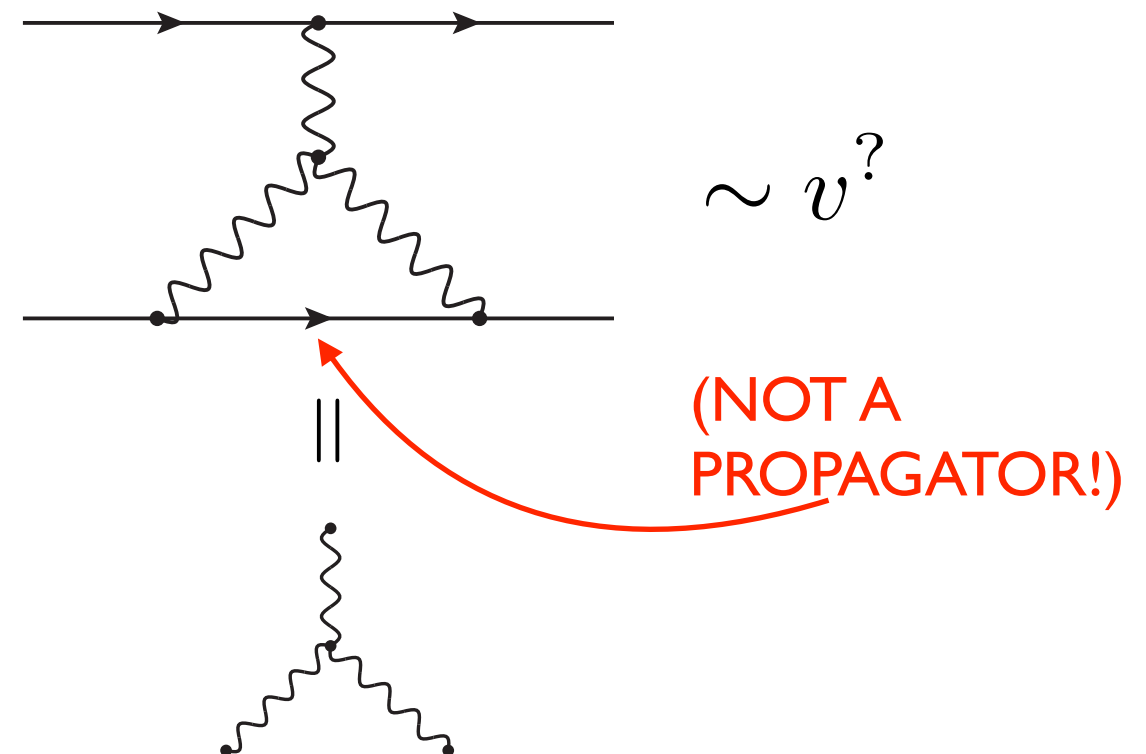
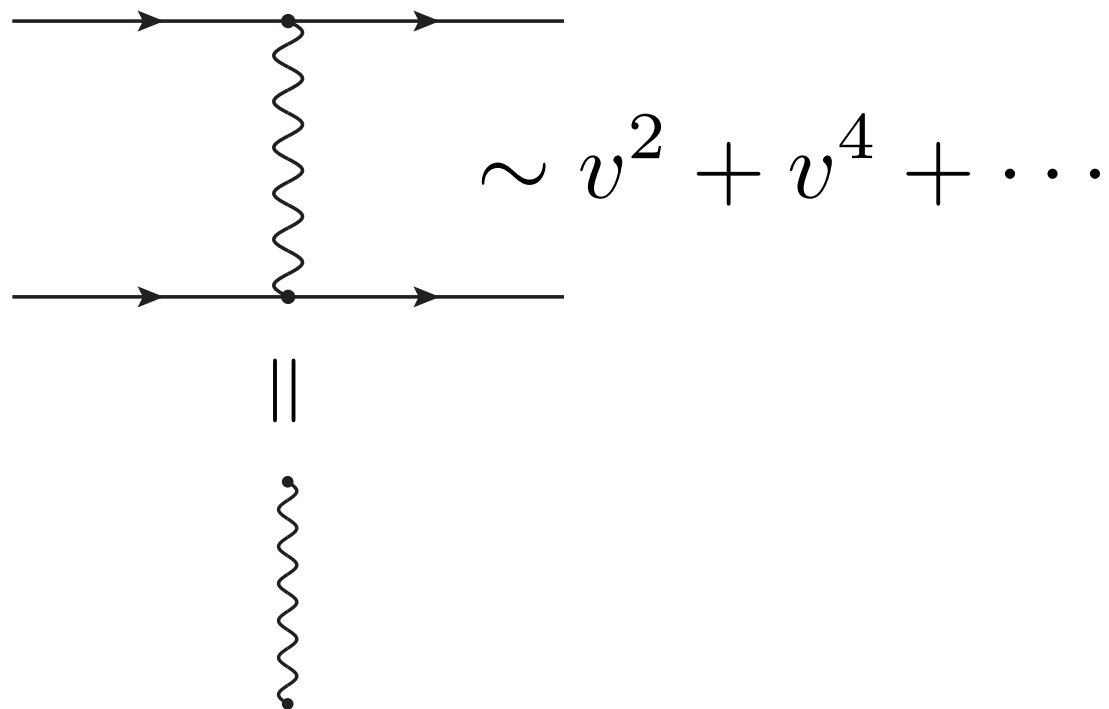
To compute the generating function  $W$  one could use standard covariant Feynman rules obtained by expanding  $S_{EH} = -2m_{Pl}^2 \int d^4x \sqrt{g} R$

$$g_{\mu\nu} = \eta_{\mu\nu} + h_{\mu\nu}/m_{Pl}$$

w/ e.g

$$\mu, \nu \text{ wavy line with } \vec{k} \rightarrow \alpha, \beta = \frac{i}{k^2} P_{\mu\nu; \alpha, \beta} \quad (\text{Feynman gauge})$$

However, these Feynman rules are not optimal for the NR limit  $v \ll 1$   
 The diagrams don't have manifest power counting in the exp. parameter:



The problem is that the diagrams involve momentum integrals over all momentum regions. However, for NR kinematics, two momentum space configurations dominate:

“potential”:  $(E \sim 0, \vec{p} \sim 1/r)$  (off-shell)

“radiation”:  $(E \sim v/r, \vec{p} \sim v/r)$

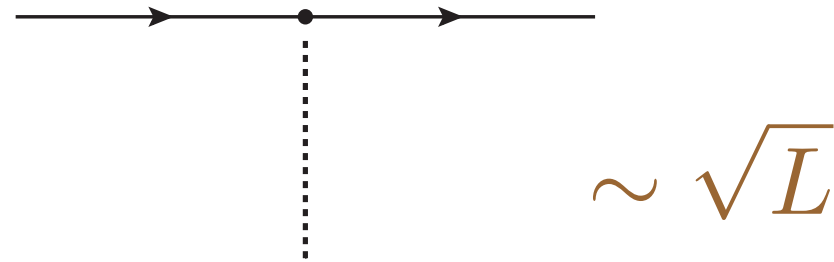
The solution to this problem is well known from NRQED/NRQCD and HQET. Decompose graviton into distinct momentum modes and “pull out” short scales:

$$g_{\mu\nu}(x) = \eta_{\mu\nu} + \bar{h}_{\mu\nu}(x) + \sum_{\mathbf{k}} e^{i\mathbf{k}\cdot\mathbf{x}} H_{\mathbf{k}\mu\nu}(x^0)$$

$\partial_\mu \bar{h} \sim \frac{v}{r} \bar{h}$ 
 $\partial_\mu H_{\mathbf{k}} \sim \frac{v}{r} H_{\mathbf{k}}$ 
 $\mathbf{k} \sim \frac{1}{r}$

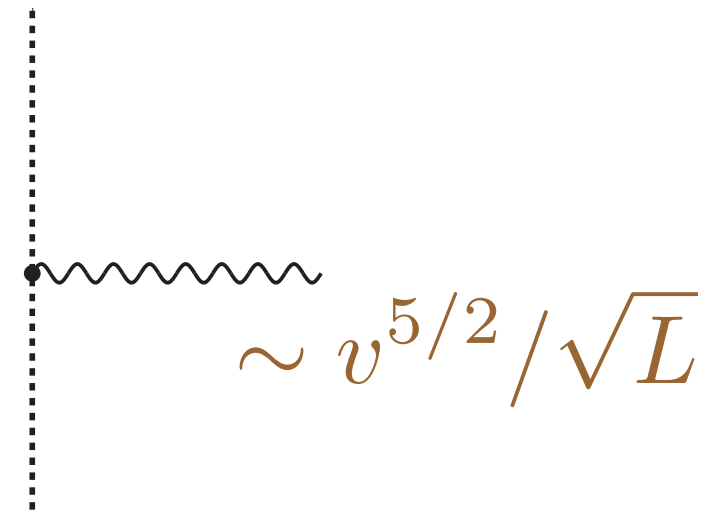
The radiation mode can be regarded as long wavelength background field in which potential gravitons propagate

In addition, need to multipole expand the couplings of the radiation mode to the particles and to the potentials. This yields an effective Lagrangian with manifest power counting in velocity:



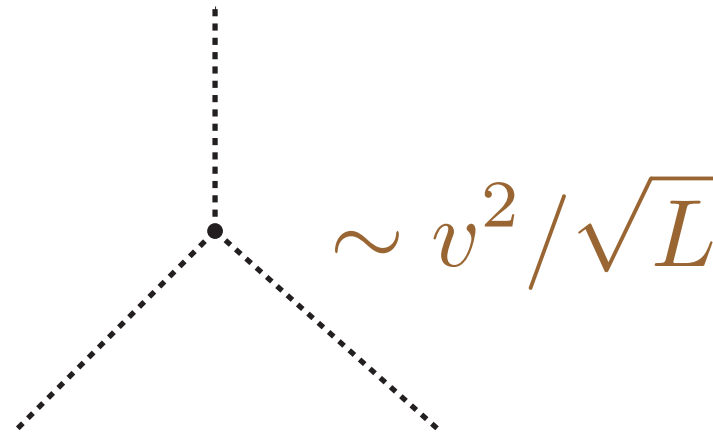
Pt. particle-Newton  
potential  
interaction:

$$\sim \sqrt{L}$$



Radiation-potential  
interaction

$$\sim v^{5/2} / \sqrt{L}$$

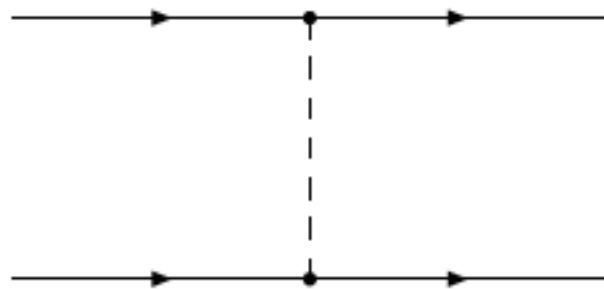


Potential graviton cubic  
self-interaction

$$\sim v^2 / \sqrt{L}$$

By connecting vertices together, generate the 2-body potentials and the interactions of matter with radiation. Drop quantum corrections  $\sim \hbar/L \ll 1$

Leading order:  
Newton  
(1687)

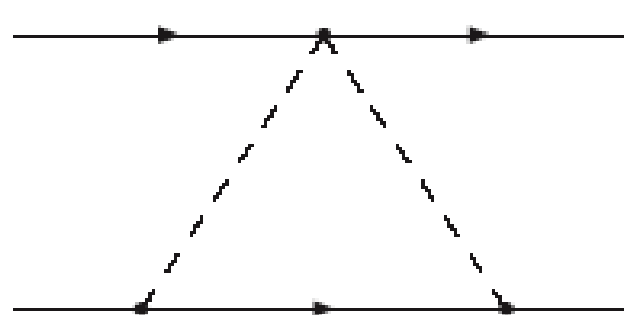
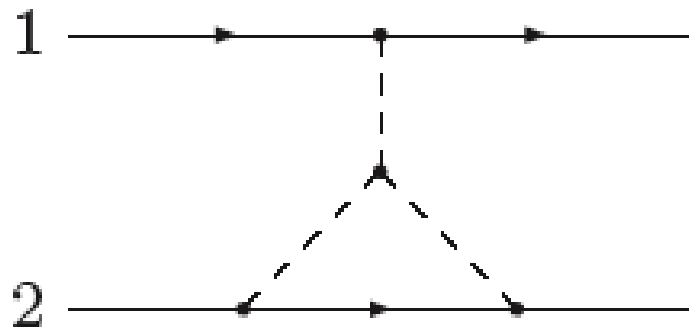
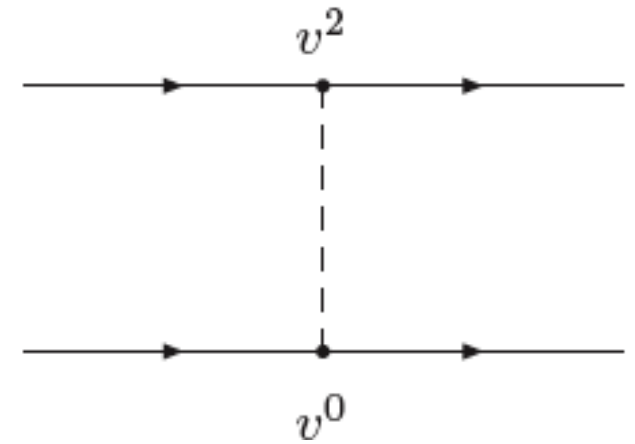
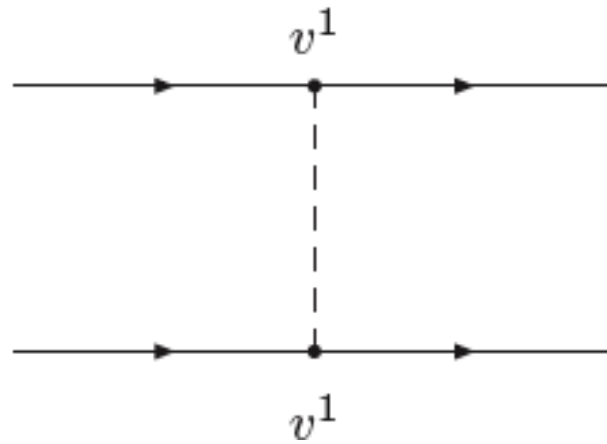
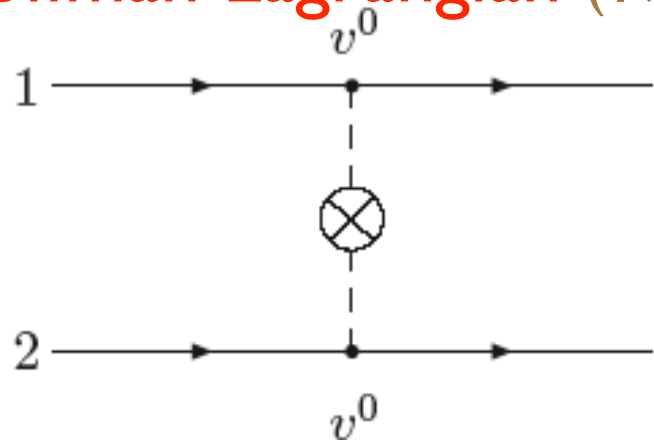


(a)



$$L = \frac{1}{2} \sum_a m_a \vec{v}_a^2 + \frac{G_N m_1 m_2}{r}$$

Next-to-leading (1PN): Einstein-Infeld  
Hoffman Lagrangian (1938)

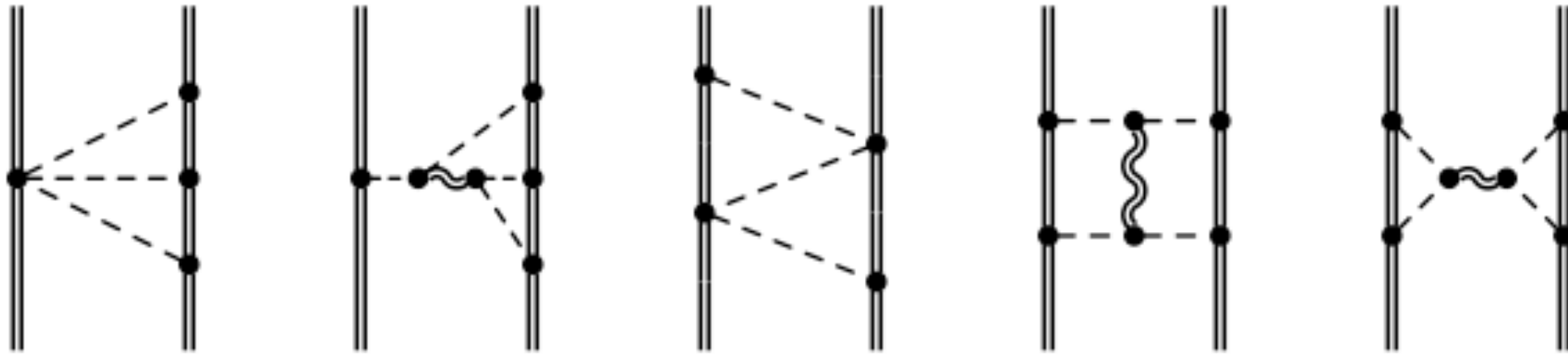


$$L_{EIH} = \frac{1}{8} \sum_a m_a \vec{v}_a^4 + \frac{G_N m_1 m_2}{2r} [3(\vec{v}_1^2 + \vec{v}_2^2) - 7\vec{v}_1 \cdot \vec{v}_2 - (\vec{v}_1 \cdot n)(\vec{v}_1 \cdot n)]$$

$$- \frac{G_N^2 m_1 m_2}{2r^2}$$

2PN (1981-2002): Some of the diagrams are

(Gilmore+Ross, PRD 2008)



$$\begin{aligned}
 L_{2PN} = & \frac{m_1 \mathbf{v}_1^6}{16} \\
 & + \frac{Gm_1 m_2}{r} \left( \frac{7}{8} \mathbf{v}_1^4 - \frac{5}{4} \mathbf{v}_1^2 \mathbf{v}_1 \cdot \mathbf{v}_2 - \frac{3}{4} \mathbf{v}_1^2 \mathbf{n} \cdot \mathbf{v}_1 \mathbf{n} \cdot \mathbf{v}_2 + \frac{3}{16} \mathbf{v}_1^2 \mathbf{v}_2^2 + \frac{1}{8} (\mathbf{v}_1 \cdot \mathbf{v}_2)^2 \right. \\
 & \quad \left. - \frac{1}{8} \mathbf{v}_1^2 (\mathbf{n} \cdot \mathbf{v}_2)^2 + \frac{3}{4} \mathbf{n} \cdot \mathbf{v}_1 \mathbf{n} \cdot \mathbf{v}_2 \mathbf{v}_1 \cdot \mathbf{v}_2 + \frac{3}{16} (\mathbf{n} \cdot \mathbf{v}_1)^2 (\mathbf{n} \cdot \mathbf{v}_2)^2 \right) \\
 & + Gm_1 m_2 \left( \frac{1}{8} \mathbf{a}_1 \cdot \mathbf{n} \mathbf{v}_2^2 + \frac{3}{2} \mathbf{a}_1 \cdot \mathbf{v}_1 \mathbf{n} \cdot \mathbf{v}_2 - \frac{7}{4} \mathbf{a}_1 \cdot \mathbf{v}_2 \mathbf{n} \cdot \mathbf{v}_2 - \frac{1}{8} \mathbf{a}_1 \cdot \mathbf{n} (\mathbf{n} \cdot \mathbf{v}_2)^2 \right) \\
 & + Gm_1 m_2 r \left( \frac{15}{16} \mathbf{a}_1 \cdot \mathbf{a}_2 - \frac{1}{16} \mathbf{a}_1 \cdot \mathbf{n} \mathbf{a}_2 \cdot \mathbf{n} \right) \\
 & + \frac{G^2 m_1 m_2^2}{r^2} \left( \frac{7}{4} \mathbf{v}_1^2 + 2 \mathbf{v}_2^2 - \frac{7}{2} \mathbf{v}_1 \cdot \mathbf{v}_2 + \frac{1}{2} (\mathbf{n} \cdot \mathbf{v}_1)^2 \right) \\
 & + \frac{G^3 m_1 m_2^3}{2r^3} + \frac{3G^3 m_1^2 m_2^2}{2r^3} + (1 \leftrightarrow 2),
 \end{aligned}$$

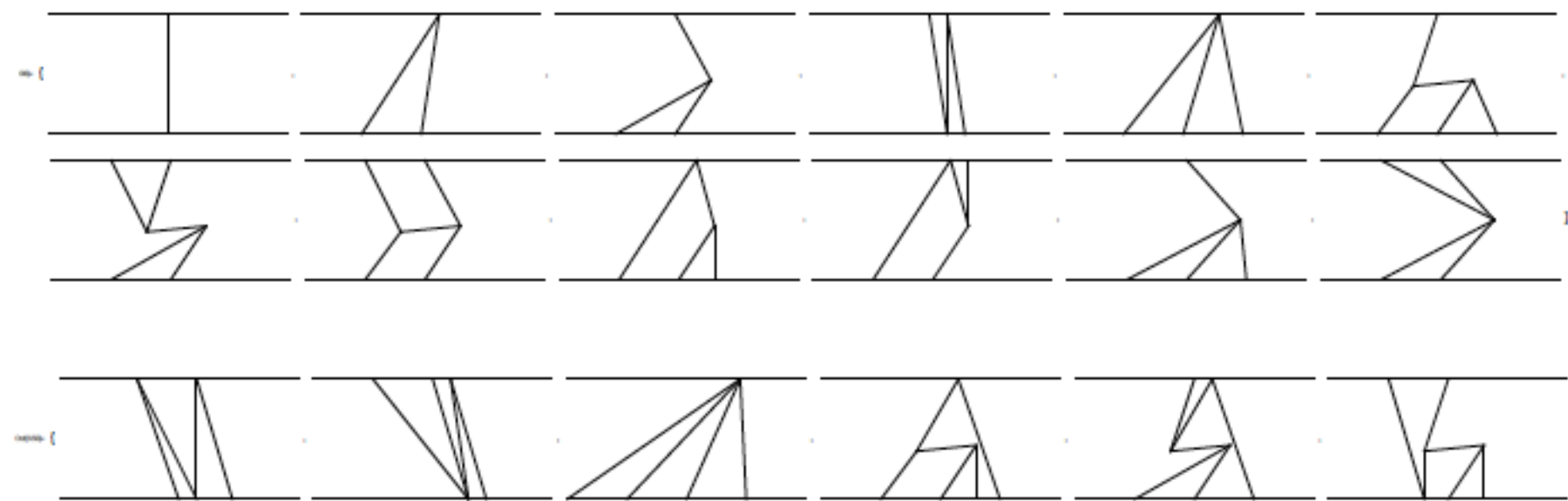
reducible to one-loop integrals via  
IBP:

$$\int \frac{d^{d-1} \mathbf{k}}{(2\pi)^{d-1}} \frac{1}{[(\mathbf{k} + \mathbf{p})^2]^\alpha [\mathbf{k}^2]^\beta}$$

(simplification of PT via field redefs:  
B. Kol+M. Smolkin, 2007-2008.)

**3PN** (1998-2003): Recently computed by Sturani+Foffa (2011). Computer generated Feynman diagrams plus table of standard Feynman integrals.

relevant topologies:



	0PN	1PN	2PN	3PN	4PN
$G$	1				
$G^2$		1	1		
$G^3$			5	4	
$G^4$				8	21
$G^5$					50

# topologies vs.  
PN order

	$v^0$	$v^2$	$v^4$	$v^6$
$G$	1	1	1	
$G^2$	1	8	7	7
$G^3$	5	48	159	...
$G^4$	8	299	...	
$G^4$	50	...		

# of diagrams/topology/  
fixed PN order.

Partial progress in EFT computation of 4PN potentials has also been made. See Sturani + Foffa, PRD 2013.



## Inclusion of BH spin into the EFT: (R. Porto, PRD 2007)

“Hyperfine” (Spin-spin) interactions: (Porto+Rothstein, PRL 2008)

$$\begin{aligned}
 V_{3PN}^{ss} = & -\frac{G_N}{2r^3} \left[ \vec{S}_1 \cdot \vec{S}_2 \left( \frac{3}{2} \vec{v}_1 \cdot \vec{v}_2 - 3 \vec{v}_1 \cdot \vec{n} \vec{v}_2 \cdot \vec{n} - (\vec{v}_1^2 + \vec{v}_2^2) \right) - \vec{S}_1 \cdot \vec{v}_1 \vec{S}_2 \cdot \vec{v}_2 - \frac{3}{2} \vec{S}_1 \cdot \vec{v}_2 \vec{S}_2 \cdot \vec{v}_1 + \vec{S}_1 \cdot \vec{v}_2 \vec{S}_2 \cdot \vec{v}_2 \right. \\
 & + \vec{S}_2 \cdot \vec{v}_1 \vec{S}_1 \cdot \vec{v}_1 + 3 \vec{S}_1 \cdot \vec{n} \vec{S}_2 \cdot \vec{n} (\vec{v}_1 \cdot \vec{v}_2 + 5 \vec{v}_1 \cdot \vec{n} \vec{v}_2 \cdot \vec{n}) - 3 \vec{S}_1 \cdot \vec{v}_1 \vec{S}_2 \cdot \vec{n} \vec{v}_2 \cdot \vec{n} - 3 \vec{S}_2 \cdot \vec{v}_2 \vec{S}_1 \cdot \vec{n} \vec{v}_1 \cdot \vec{n} \\
 & + 3(\vec{v}_2 \times \vec{S}_1) \cdot \vec{n} (\vec{v}_2 \times \vec{S}_2) \cdot \vec{n} + 3(\vec{v}_1 \times \vec{S}_1) \cdot \vec{n} (\vec{v}_1 \times \vec{S}_2) \cdot \vec{n} - \frac{3}{2} (\vec{v}_1 \times \vec{S}_1) \cdot \vec{n} (\vec{v}_2 \times \vec{S}_2) \cdot \vec{n} \\
 & \left. - 6(\vec{v}_1 \times \vec{S}_2) \cdot \vec{n} (\vec{v}_2 \times \vec{S}_1) \cdot \vec{n} \right] + \frac{3G_N^2(m_1 + m_2)}{r^4} (\vec{S}_1 \cdot \vec{S}_2 - 3 \vec{S}_1 \cdot \vec{n} \vec{S}_2 \cdot \vec{n}),
 \end{aligned}$$

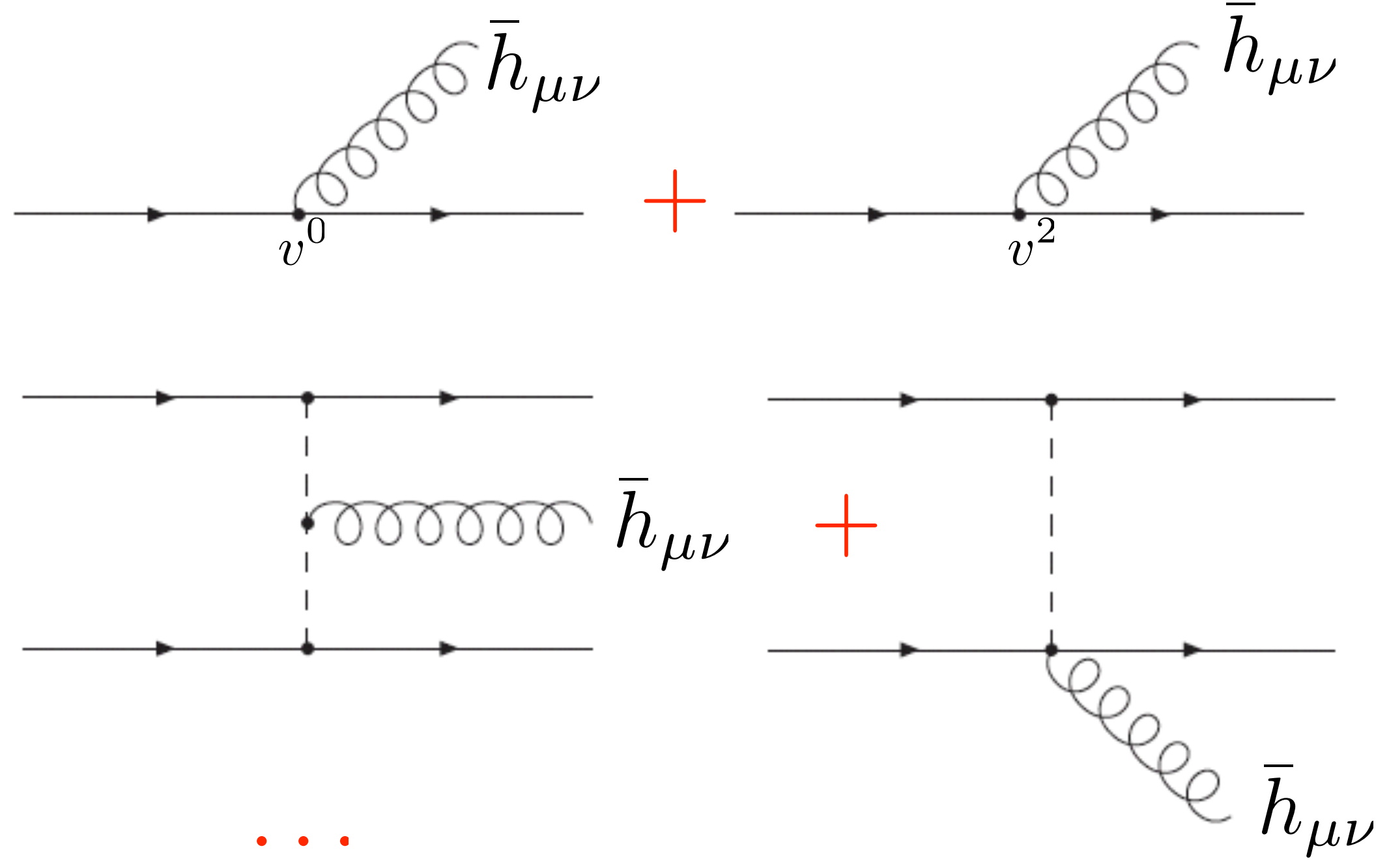
$\vec{S}^2$ —orbit couplings: (Porto+Rothstein, PRD 2008)

$$\begin{aligned}
 & = C_{ES^2}^{(1)} \frac{G_N m_2}{2m_1 r^3} [S_1^{j0} S_1^{i0} (3n^i n^j - \delta^{ij}) - 2S_1^{k0} ((\mathbf{v}_1 \times \mathbf{S}_1)^k - 3(\mathbf{n} \cdot \mathbf{v}_1)(\mathbf{n} \times \mathbf{S}_1)^k)] \\
 & + C_{ES^2}^{(1)} \frac{G_N m_2}{2m_1 r^3} \left[ \mathbf{S}_1^2 \left( 6(\mathbf{n} \cdot \mathbf{v}_1)^2 - \frac{15}{2} \mathbf{n} \cdot \mathbf{v}_1 \mathbf{n} \cdot \mathbf{v}_2 + \frac{13}{2} \mathbf{v}_1 \cdot \mathbf{v}_2 - \frac{3}{2} \mathbf{v}_2^2 - \frac{7}{2} \mathbf{v}_1^2 \right) \right. \\
 & + (\mathbf{S}_1 \cdot \mathbf{n})^2 \left( \frac{9}{2} (\mathbf{v}_1^2 + \mathbf{v}_2^2) - \frac{21}{2} \mathbf{v}_1 \cdot \mathbf{v}_2 - \frac{15}{2} \mathbf{n} \cdot \mathbf{v}_1 \mathbf{n} \cdot \mathbf{v}_2 \right) + 2\mathbf{v}_1 \cdot \mathbf{S}_1 \mathbf{v}_1 \cdot \mathbf{S}_1 \\
 & \left. - 3\mathbf{v}_1 \cdot \mathbf{S}_1 \mathbf{v}_2 \cdot \mathbf{S}_1 - 6\mathbf{n} \cdot \mathbf{v}_1 \mathbf{n} \cdot \mathbf{S}_1 \mathbf{v}_1 \cdot \mathbf{S}_1 + 9\mathbf{n} \cdot \mathbf{v}_2 \mathbf{n} \cdot \mathbf{S}_1 \mathbf{v}_1 \cdot \mathbf{S}_1 + 3\mathbf{n} \cdot \mathbf{v}_1 \mathbf{n} \cdot \mathbf{S}_1 \mathbf{v}_2 \cdot \mathbf{S}_1 \right] \\
 & - C_{ES^2}^{(1)} \frac{m_2 G_N}{2m_1 r^3} (\mathbf{S}_1^2 - 3(\mathbf{S}_1 \cdot \mathbf{n})^2) + C_{ES^2}^{(1)} \frac{m_2 G_N^2}{2r^4} \left( 1 + \frac{4m_2}{m_1} \right) (\mathbf{S}_1^2 - 3(\mathbf{S}_1 \cdot \mathbf{n})^2) \\
 & - \frac{G_N^2 m_2}{r^4} (\mathbf{S}_1 \cdot \mathbf{n})^2 + (\tilde{\mathbf{a}}_{1(1)}^{so})^l S_1^{0l} + \mathbf{v}_1 \times \mathbf{S}_1 \cdot \tilde{\mathbf{a}}_{1(1)}^{so} + 1 \leftrightarrow 2.
 \end{aligned}$$

=I for BH

# One graviton sector: radiation couplings (WVG+A. Ross, PRD 2010)

Integrating out potential modes gives the couplings of 2-body system to radiation:

$$T^{\mu\nu} =$$


The equation shows a sum of Feynman diagrams representing the coupling of a two-body system to a graviton. The first row contains two diagrams separated by a red plus sign. The first diagram shows a horizontal line with an arrow pointing right, with a vertex labeled  $v^0$  from which a wavy line labeled  $\bar{h}_{\mu\nu}$  goes up and to the right. The second diagram shows a similar horizontal line with a vertex labeled  $v^2$  from which a wavy line labeled  $\bar{h}_{\mu\nu}$  goes up and to the right. The second row contains two diagrams separated by a red plus sign. The first diagram shows two horizontal lines with arrows pointing right, connected by a vertical dashed line. A wavy line labeled  $\bar{h}_{\mu\nu}$  is attached to the vertical dashed line. The second diagram shows two horizontal lines with arrows pointing right, connected by a vertical dashed line. A wavy line labeled  $\bar{h}_{\mu\nu}$  is attached to the bottom of the vertical dashed line. Below the second row is a red plus sign followed by three red dots, indicating further terms in the series.

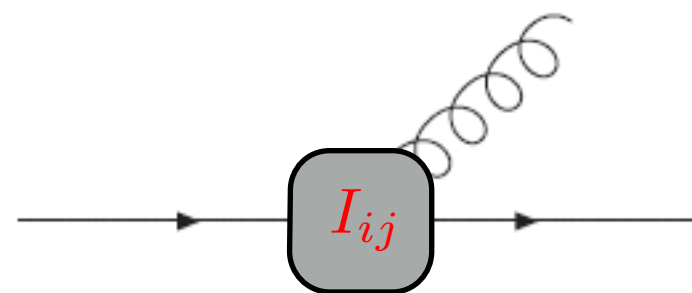
(1st graph=LO. Last three graphs are NLO).

The resulting action consists of a set of multipole moments coupled to the worldline of composite object. In the CM frame,

$$\Gamma[\bar{h}] = \frac{1}{2m_{Pl}} \int dx^0 \left[ I_E^{ij}(x^0) R_{0i0j} + \frac{4}{3} I_B^{i,jk}(x^0) R_{0jik} + \frac{1}{3} I_E^{ijk}(x^0) \nabla_k R_{0i0j} + \cdots \right]$$

$\ell = 2_E$        $\ell = 2_B$        $\ell = 3_E$

For example, the quadrupole moment to NLO (Will+Wagoner, 1970's)

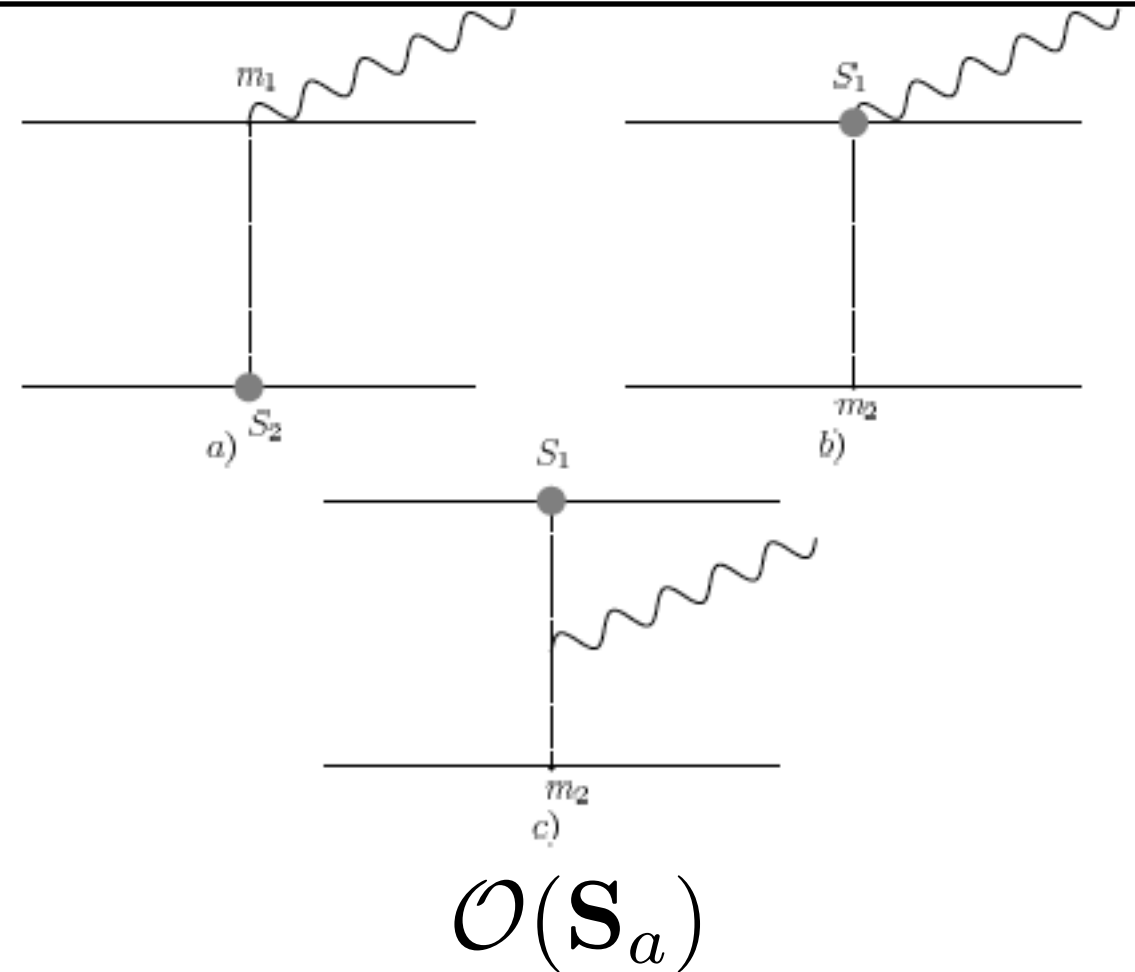
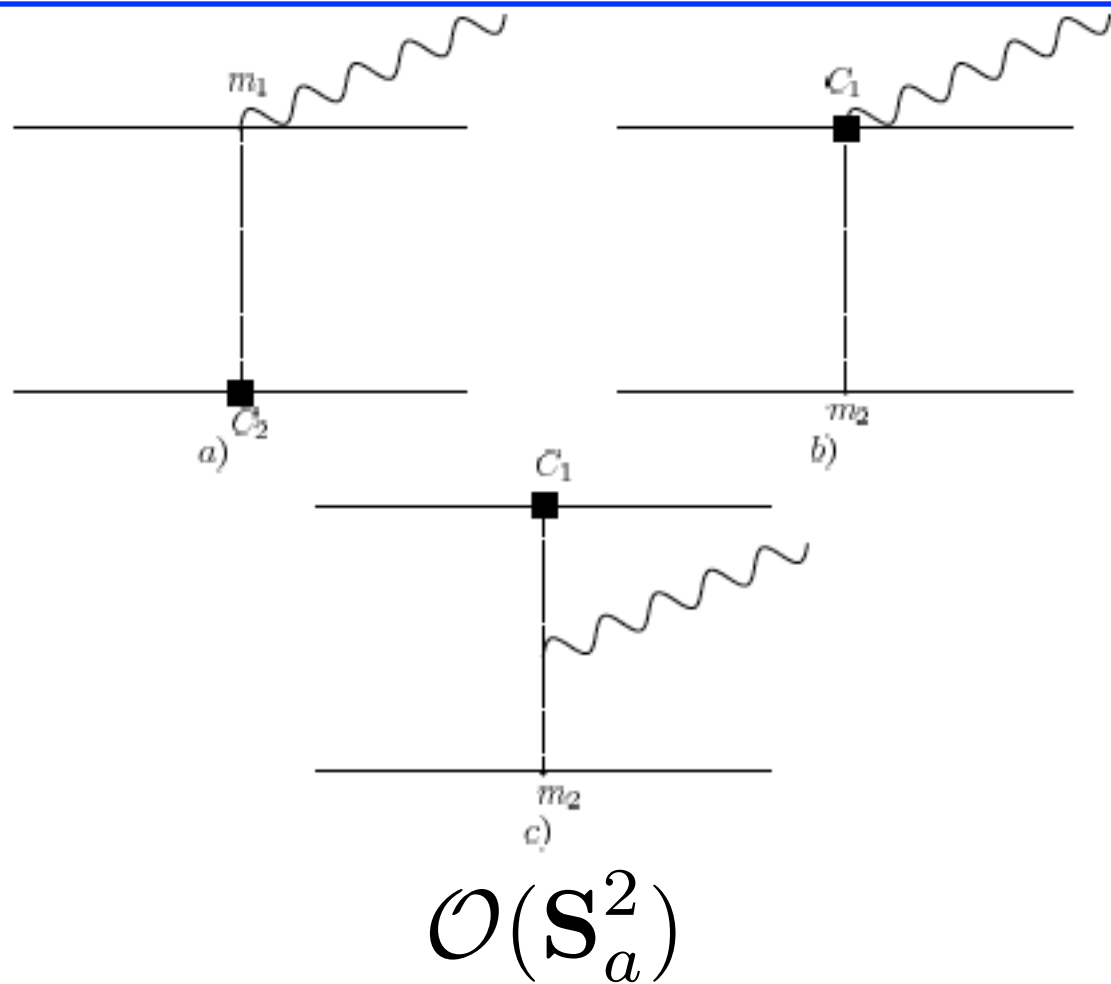
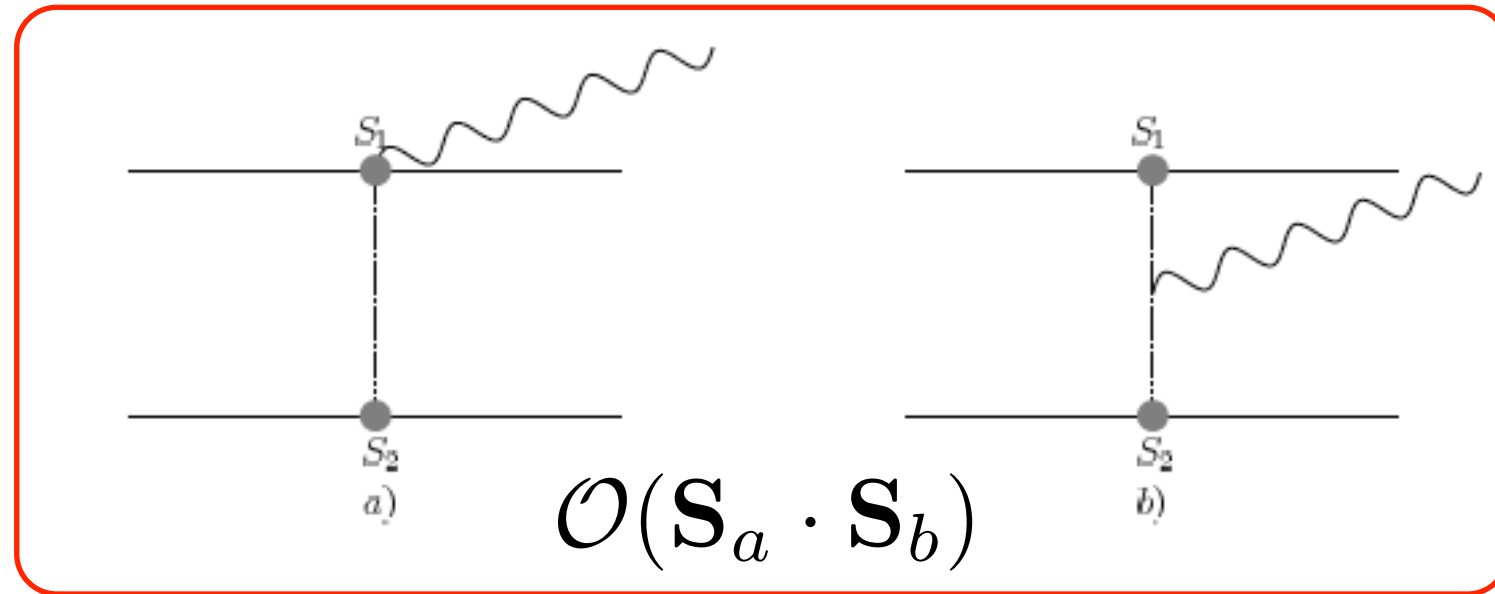


$$= \int d^3\mathbf{x} \left[ T^{00} + T^{aa} + \frac{11}{42} \mathbf{x}^2 \ddot{T}^{00} - \frac{4}{3} \dot{T}^{0k} x^k \right] [x^i x^j]^{TF} + \mathcal{O}(v^4)$$

$$= \sum_a m_a \mathbf{x}_a^i \mathbf{x}_a^j \left[ 1 + \frac{3}{2} \mathbf{v}_a^2 - \sum_b \frac{G_N m_b}{|\mathbf{x}_a - \mathbf{x}_b|} \right] + \frac{11}{42} \sum_a m_a \frac{d^2}{dt^2} (\mathbf{x}_a^2 \mathbf{x}_a^i \mathbf{x}_a^j)$$

$$- \frac{4}{3} \sum_a m_a \frac{d}{dt} (\mathbf{x}_a \cdot \mathbf{v}_a \mathbf{x}_a^i \mathbf{x}_a^j) - \text{traces} + \mathcal{O}(v^4)$$

This formalism has been used recently to compute spin-induced moments  
at 3PN order (Porto+Ross+Rothstein 2011)



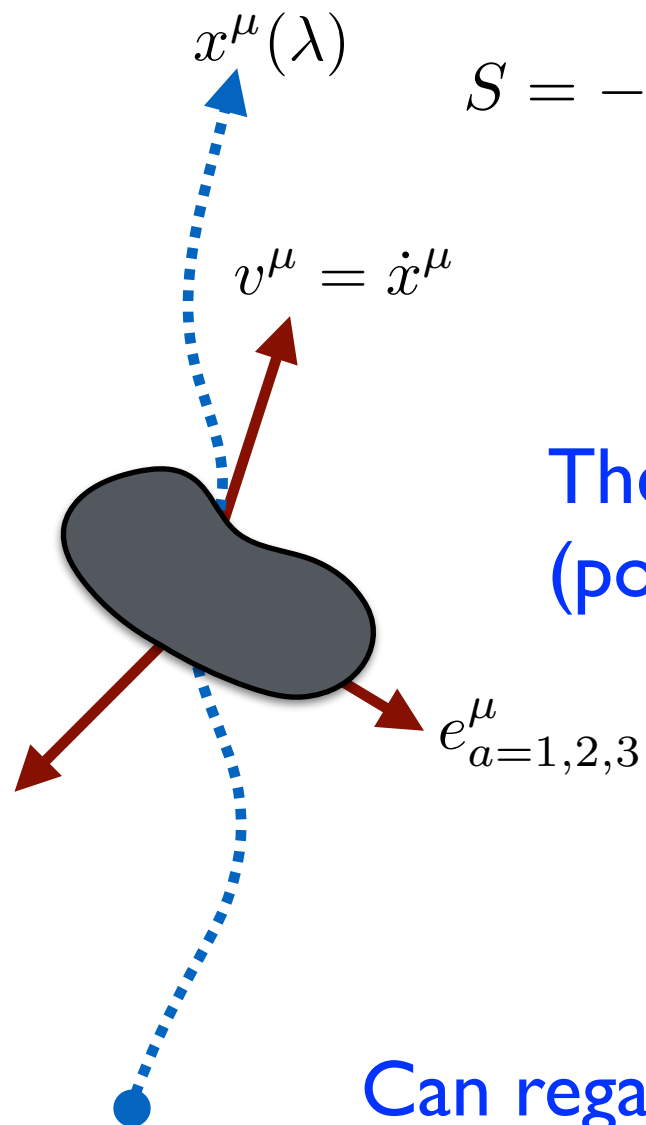
# EFTIII: Radiation

(Double expansion:  $\eta_2 = r/\lambda \sim v$   
 $\eta_3 = r/r_g \sim v^3$  )

(WG+Ross, PRD 2010)

This is a field theory of radiation coupled to a point object with multipole moments. Most general diff. invariant action:

$$S = - \int d\tau(\lambda) m(\lambda) - \int dx^\mu L_{ab}(\lambda) \omega_\mu^{ab}(x(\tau)) + \frac{1}{2} \int d\tau(\lambda) I_{ab}(\lambda) E^{ab}(x(\tau)) \\ - \frac{2}{3} \int d\tau J_{ab}(\lambda) B^{ab}(x) + \frac{1}{6} \int d\tau I_{abc}(\lambda) \nabla^c E^{ab}(x) + \dots$$



The time evolution of the moments arises from short dist. (potentials) as well as radiative corrections (radiation reaction).

Can regard the moments as time-dependent **Wilson coefficients** (coupling constants). Radiative corrections in the EFT will generate **RG flows** for them.

Can use this theory to compute observables at infinity, even if the short distance time evolution of the moments is not known. For example, the graviton emission amplitude involving the 1st three moments:

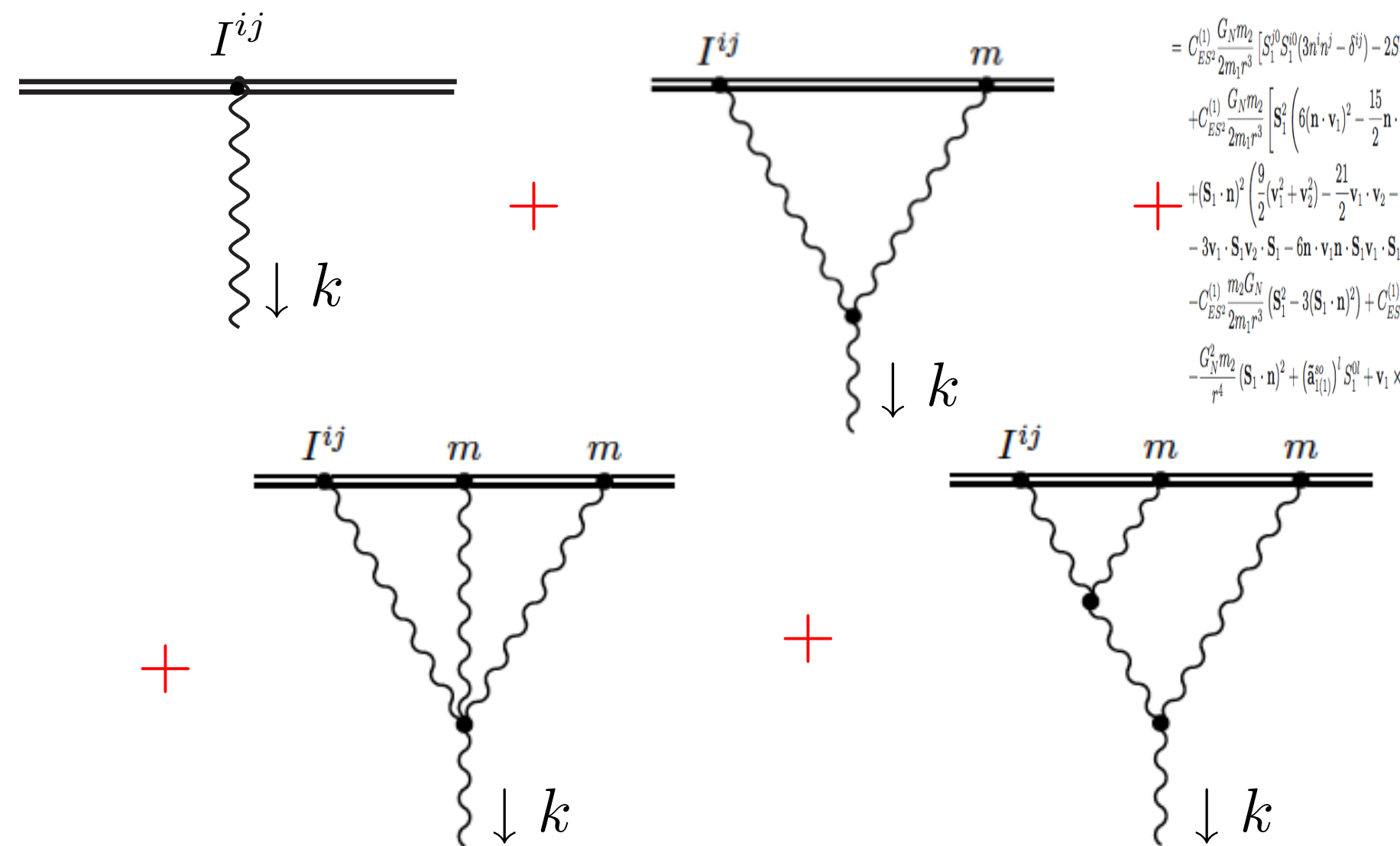
$$\begin{aligned}
 i\mathcal{A}_h(\mathbf{k}) &= \text{diagram with } I^{ij} \text{ and wavy line} + \text{diagram with } J^{ij} \text{ and wavy line} + \text{diagram with } I^{ijk} \text{ and wavy line} + \dots \\
 &= \frac{i}{4m_{Pl}} \epsilon_{ij}^*(\mathbf{k}, h) \left[ \mathbf{k}^2 I^{ij}(k) + \frac{4}{3} |\mathbf{k}| k^l \epsilon^{ikl} J^{jk}(k) - \frac{i}{3} \mathbf{k}^2 k^l I^{ijl}(k) + \dots \right]
 \end{aligned}$$

Determines the time averaged energy loss rate of the composite system:

$$\dot{P}^0 = \frac{G_N}{5} \left\langle \left( \frac{d^3}{dt^3} I^{ij}(t) \right)^2 \right\rangle + \frac{16G_N}{45} \left\langle \left( \frac{d^3}{dt^3} J^{ij}(t) \right)^2 \right\rangle + \frac{G_N}{189} \left\langle \left( \frac{d^4}{dt^4} I^{ijk}(t) \right)^2 \right\rangle + \dots$$

# UV and IR divergences in radiation

Focus on the  $\ell = 2$  channel. The amplitude to second order is

$$i\mathcal{A}(k) =$$


$$= C_{ES^2}^{(1)} \frac{G_N m_2}{2m_1 r^3} \left[ S_1^{j0} S_1^{i0} (3n^i n^j - \delta^{ij}) - 2S_1^{kl} \left( (\mathbf{v}_1 \times \mathbf{S}_1)^k - 3(\mathbf{n} \cdot \mathbf{v}_1)(\mathbf{n} \times \mathbf{S}_1)^k \right) \right]$$

$$+ C_{ES^2}^{(1)} \frac{G_N m_2}{2m_1 r^3} \left[ S_1^2 \left( 6(\mathbf{n} \cdot \mathbf{v}_1)^2 - \frac{15}{2} \mathbf{n} \cdot \mathbf{v}_1 \mathbf{n} \cdot \mathbf{v}_2 + \frac{13}{2} \mathbf{v}_1 \cdot \mathbf{v}_2 - \frac{3}{2} v_2^2 - \frac{7}{2} v_1^2 \right) \right.$$

$$+ (\mathbf{S}_1 \cdot \mathbf{n})^2 \left( \frac{9}{2} (v_1^2 + v_2^2) - \frac{21}{2} \mathbf{v}_1 \cdot \mathbf{v}_2 - \frac{15}{2} \mathbf{n} \cdot \mathbf{v}_1 \mathbf{n} \cdot \mathbf{v}_2 \right) + 2\mathbf{v}_1 \cdot \mathbf{S}_1 \mathbf{v}_1 \cdot \mathbf{S}_1$$

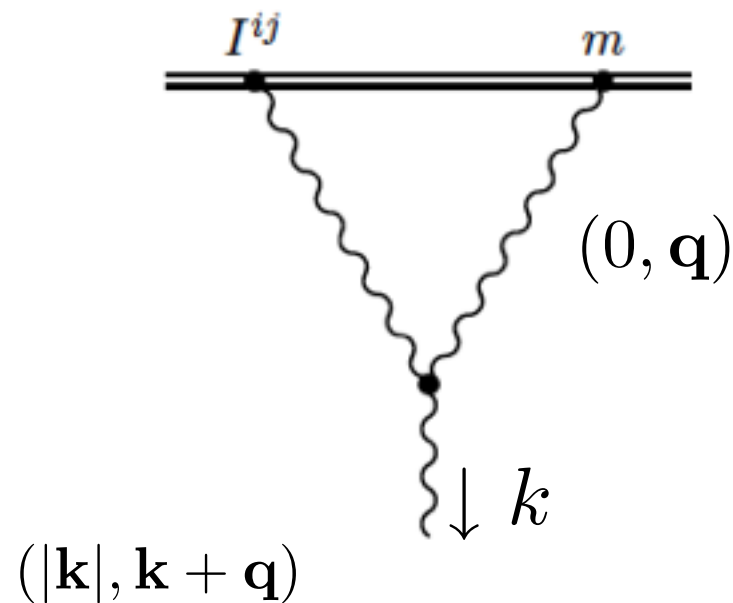
$$- 3\mathbf{v}_1 \cdot \mathbf{S}_1 \mathbf{v}_2 \cdot \mathbf{S}_1 - 6\mathbf{n} \cdot \mathbf{v}_1 \mathbf{n} \cdot \mathbf{S}_1 \mathbf{v}_1 \cdot \mathbf{S}_1 + 9\mathbf{n} \cdot \mathbf{v}_2 \mathbf{n} \cdot \mathbf{S}_1 \mathbf{v}_1 \cdot \mathbf{S}_1 + 3\mathbf{n} \cdot \mathbf{v}_1 \mathbf{n} \cdot \mathbf{S}_1 \mathbf{v}_2 \cdot \mathbf{S}_1 \Big]$$

$$- C_{ES^2}^{(1)} \frac{m_2 G_N}{2m_1 r^3} (S_1^2 - 3(\mathbf{S}_1 \cdot \mathbf{n})^2) + C_{ES^2}^{(1)} \frac{m_2 G_N^2}{2r^4} \left( 1 + \frac{4m_2}{m_1} \right) (S_1^2 - 3(\mathbf{S}_1 \cdot \mathbf{n})^2)$$

$$- \frac{G_N^2 m_2}{r^4} (\mathbf{S}_1 \cdot \mathbf{n})^2 + (\tilde{\mathbf{a}}_{1(l)}^{so})^l S_1^{0l} + \mathbf{v}_1 \times \mathbf{S}_1 \cdot \tilde{\mathbf{a}}_{1(l)}^{so} + \dots \downarrow k$$

Non-linear interaction of emitted gravitons with multipole moments introduces both UV and IR divergences.

Leading IR divergence: The order  $\eta_3 \sim v^3$  correction to the amplitude:



Can be reduced to scalar Feynman integrals of the form

$$I_n(|\mathbf{k}|) = \int \frac{d^{d-1}\mathbf{q}}{(2\pi)^{d-1}} \frac{(\mathbf{q}^2)^n}{\mathbf{k}^2 - (\mathbf{k} + \mathbf{q})^2 + i\epsilon}$$

$$(n \geq -1)$$

Note that for  $n = -1$  this has an infrared divergence.

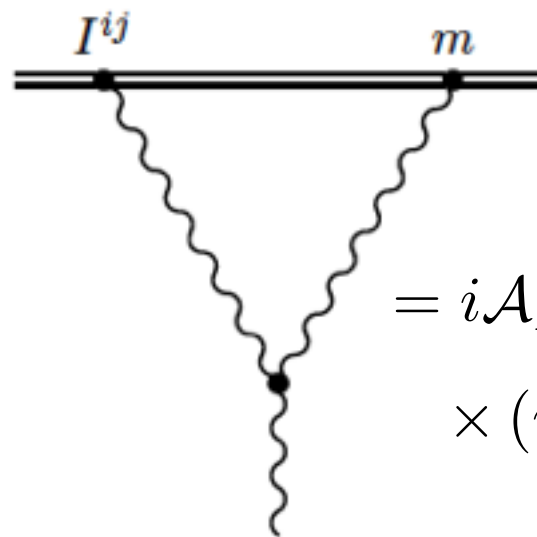
As  $\mathbf{q} \rightarrow 0$  ( $d = 4 - 2\epsilon$ )

$$I_{-1}(|\mathbf{k}|) = \int \frac{d^{d-1}\mathbf{q}}{(2\pi)^{d-1}} \frac{1}{\mathbf{q}^2} \frac{1}{\mathbf{k}^2 - (\mathbf{k} + \mathbf{q})^2 + i\epsilon} \sim \int \frac{d^3\mathbf{q}}{(2\pi)^3} \frac{1}{\mathbf{q}^2(\mathbf{k} \cdot \mathbf{q})} \sim \frac{1}{\epsilon_{IR}}$$

Physically, this is the familiar “Coulomb” singularity: nearly on-shell graviton interacts with the long range  $1/r$  potential of the composite object.



The complete result is



$$= i\mathcal{A}_{LO} \times (iG_N m |\mathbf{k}|) \left[ -\frac{(\mathbf{k}^2 + i\epsilon)}{\pi\mu^2} e^{\gamma_E} \right]^{(d-4)/2} \times \left[ \frac{2}{(d-4)_{IR}} - \frac{11}{6} + (d-4) \left( \frac{\pi^2}{8} + \frac{203}{72} \right) \right]$$

Note that to order  $G_N m |\mathbf{k}| \sim v^3$ , the IR singularities drop from  $|\mathcal{A}|^2$

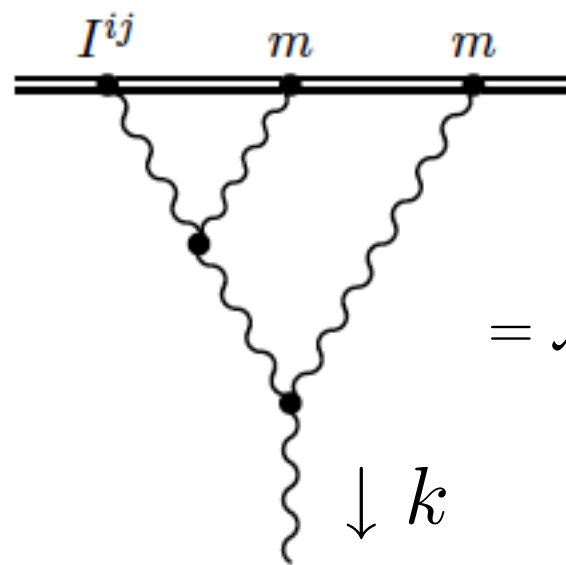
$$\left| \frac{\mathcal{A}}{\mathcal{A}_{LO}} \right|^2 = 1 + 2G_N m |\mathbf{k}| + \mathcal{O}(1/\epsilon_{IR}^2)$$

The “Coulomb tail” is responsible for non-analytic corrections to the radiated power in gravitons. Eg,

$$P_{v^3} = P_{LO} \times (4\pi v^3) \qquad P_{v^5} = P_{LO} \times \left( -\frac{8191}{672} \pi v^5 \right)$$

## Subleading IR divergences:

The following order  $\eta_3^2 \sim v^6$  diagram is also IR divergent by power counting



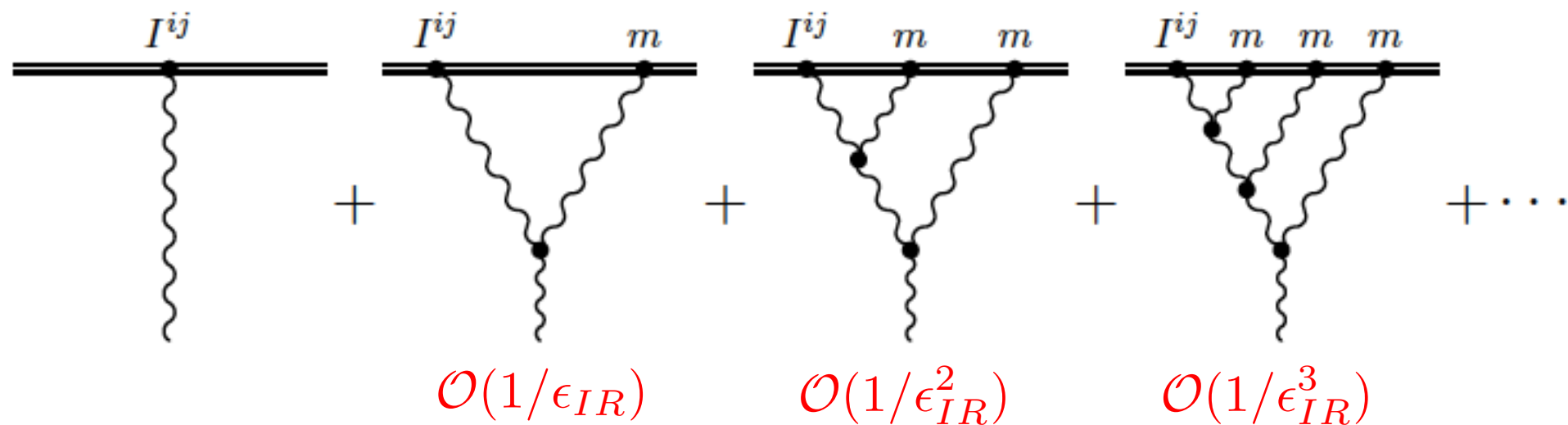
$$= \mathcal{A}_{LO} (G_N m |\mathbf{k}|)^2 \left[ -\frac{(\mathbf{k}^2 + i\epsilon)}{\pi \mu^2} e^{\gamma_E} \right]^{(d-4)} \times \left[ -\frac{2}{(d-4)_{IR}^2} + \frac{11}{3} \frac{1}{(d-4)_{IR}} + \dots \right]$$

but one can check that all IR divergences cancel out of physical quantities, up to higher order terms in perturbation theory. E.g:

$$\left| \mathcal{A}_{\mathcal{O}(\eta_3^2)} \right|^2 = \left| \text{Diagram} \right|^2 + 2 \operatorname{Re} \left( \text{Diagram} \right)$$

is independent of  $1/\epsilon_{IR}$

We also showed that the leading  $1/\epsilon_{IR}$  poles at each order, from the diagrams



sum up to a complex phase in the emission amplitude,

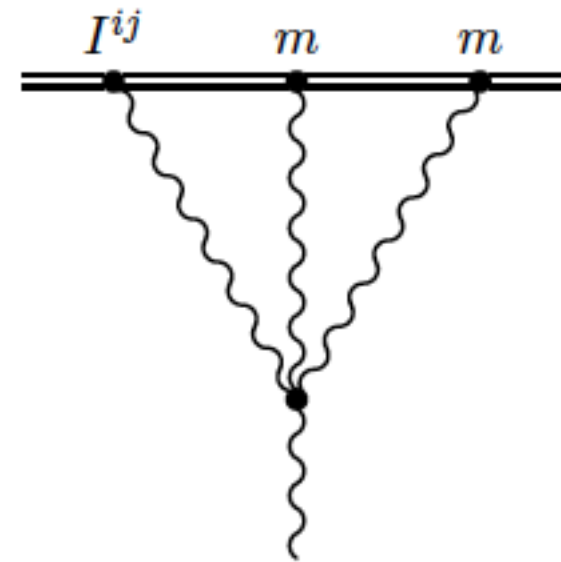
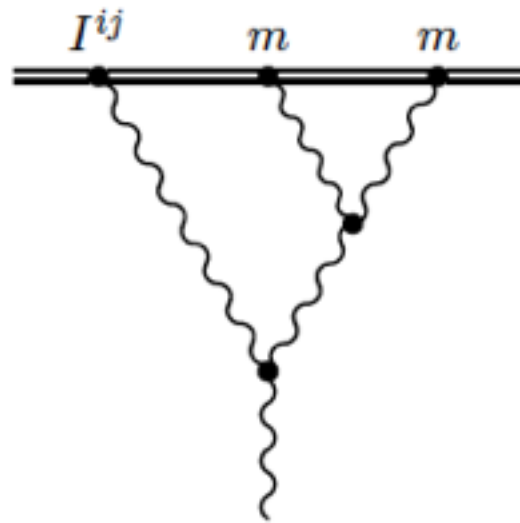
$$\mathcal{A} = \exp \left[ \frac{2iG_N m \omega}{(d-4)_{IR}} \right] \mathcal{A}_{\text{finite}} \rightarrow |\mathcal{A}|^2 = \text{IR finite}$$

so poles drop out of physical predictions.

The handling of IR divergences in the waveform  $h_{ij}^{TT}(t, \mathbf{x} \rightarrow \infty)$  has been recently addressed. (Porto, Ross, Rothstein, arXiv 1203.2962).

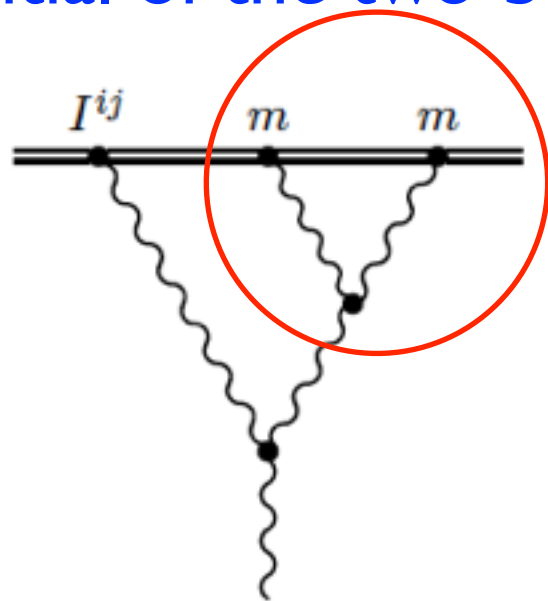
# Leading UV divergences

The following graphs at order  $\eta_3^2 \sim v^6$



are logarithmically UV divergent.

This reflects the interaction of nearly on-shell outgoing graviton with the  $1/r^2$  potential of the two-body system. Eg.



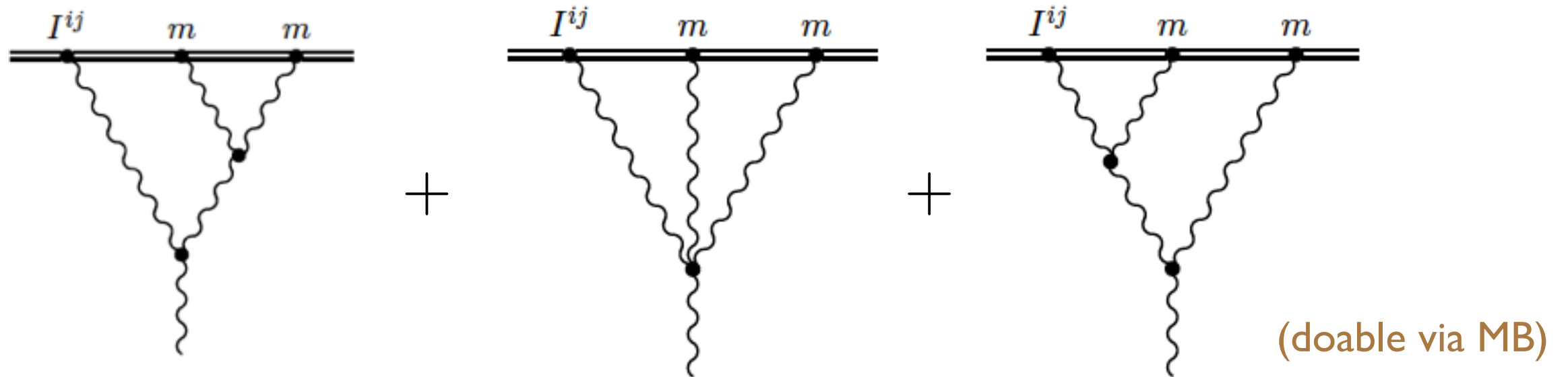
$$\sim \frac{1}{|\mathbf{q}|}$$



$$\int \frac{d^d \mathbf{q}}{(2\pi)^d} \frac{1}{|\mathbf{q}|} \frac{1}{\mathbf{k}^2 - (\mathbf{k} + \mathbf{q})^2 + i\epsilon}$$

$$\sim \int \frac{d^3 \mathbf{q}}{(2\pi)^3} \frac{1}{|\mathbf{q}|^3} \sim \frac{1}{\epsilon_{UV}}$$

The full result at second order in the expansion is then



$$\frac{\mathcal{A}_{\eta^2}}{\mathcal{A}_{\eta^0}} = (G_N m |\mathbf{k}|)^2 \left[ -\frac{(\mathbf{k}^2 + i\epsilon)}{\pi\mu^2} e^{\gamma_E} \right]^{-2\epsilon} \times \left[ -\frac{1}{2\epsilon_{IR}^2} - \frac{11}{6} \frac{1}{\epsilon_{IR}} + \frac{107}{210} \frac{1}{\epsilon_{UV}} - \frac{7\pi^2}{12} - \frac{1777}{14700} \right].$$

# RG flows

UV divergences correspond to singularities in the multipole expansion, first at  $\eta_3^2 \sim v^6$ . In the EFT, these divergences are absorbed into the Wilson coefficients, i.e, **renormalization of the multipole moments**

$$\mu \frac{d}{d\mu} I_{ij}^R(\omega, \mu) = -\frac{214}{105} (G_N m \omega)^2 I_{ij}^R(\omega, \mu),$$



$$I_{ij}(\omega, \mu) = \left[ \frac{\mu}{\mu_0} \right]^{-\frac{214}{105} (G_N m \omega)^2} I_{ij}(\omega, \mu_0).$$

This can be used to predict the pattern of logs  $\sim \eta^{2n} \log^n \eta$  in quadrupole radiation:

$$\left| \frac{\mathcal{A}(\omega)}{\mathcal{A}_{\eta^0}(\omega, \mu_0)} \right|_{\text{leading log}}^2 = 1 - \frac{428}{105} (G_N m \omega)^2 \ln \frac{\omega}{\mu_0} + \frac{91592}{11025} (G_N m \omega)^4 \ln^2 \frac{\omega}{\mu_0} - \frac{39201376}{3472875} (G_N m \omega)^6 \ln^3 \frac{\omega}{\mu_0} + \dots$$

For circular orbits, our prediction is

$$\frac{\dot{E}_{LL}}{\dot{E}_{LO}} = v^{-\frac{1712}{105}v^6} = 1 - \frac{1712}{105}v^6 \ln v + \frac{1465472}{11025}v^{12} \ln^2 v - \frac{2508888064}{3472875}v^{18} \ln^3 v + \dots$$

This was confirmed recently by BH perturbation theory (R. Fujita, arXiv:1211.5535)

$$\begin{aligned} \frac{dE}{dt} = & \left( \frac{dE}{dt} \right)_N \left[ 1 - \frac{1247}{336}v^2 + 4\pi v^3 - \frac{44711}{9072}v^4 - \frac{8191}{672}\pi v^5 \right. \\ & + \left\{ \frac{6643739519}{69854400} - \frac{1712}{105}\gamma - \frac{3424}{105}\ln(2) + \frac{16}{3}\pi^2 - \frac{1712}{105}\ln(v) \right\} v^6 - \frac{16285}{504}\pi v^7 \\ & + \left\{ -\frac{323105549467}{3178375200} + \frac{232597}{4410}\gamma + \frac{39931}{294}\ln(2) - \frac{1369}{126}\pi^2 - \frac{47385}{1568}\ln(3) \right. \\ & \quad \left. + \frac{232597}{4410}\ln(v) \right\} v^8 \\ & + \left\{ \frac{265978667519}{745113600}\pi - \frac{13696}{105}\ln(2)\pi - \frac{6848}{105}\pi\gamma - \frac{6848}{105}\pi\ln(v) \right\} v^9 \\ & + \left\{ -\frac{2500861660823683}{2831932303200} + \frac{916628467}{7858620}\gamma - \frac{83217611}{1122660}\ln(2) - \frac{424223}{6804}\pi^2 \right. \\ & \quad \left. + \frac{47385}{196}\ln(3) + \frac{916628467}{7858620}\ln(v) \right\} v^{10} \\ & + \left\{ \frac{177293}{1176}\pi\gamma + \frac{8521283}{17640}\ln(2)\pi + \frac{8399309750401}{101708006400}\pi - \frac{142155}{784}\pi\ln(3) + \frac{177293}{1176}\pi\ln(v) \right\} v^{11} \\ & + \left\{ -\frac{256}{45}\pi^4 - \frac{37744140625}{260941824}\ln(5) + \frac{2067586193789233570693}{602387400044430000} \right. \\ & \quad - \frac{246137536815857}{157329572400}\gamma - \frac{27392}{105}\zeta(3) - \frac{437114506833}{789268480}\ln(3) \\ & \quad - \frac{271272899815409}{157329572400}\ln(2) + \frac{5861888}{11025}\ln(2)\gamma - \frac{54784}{315}\ln(2)\pi^2 \\ & \quad + \frac{3803225263}{10478160}\pi^2 - \frac{27392}{315}\pi^2\gamma + \frac{5861888}{11025}\ln(2)^2 + \frac{1465472}{11025}\gamma^2 \\ & \quad + \left( \frac{2938944}{11025}\gamma - \frac{27392}{315}\pi^2 - \frac{246137536815857}{157329572400} + \frac{5861888}{11025}\ln(2) \right) \ln(v) \\ & \quad \left. + \frac{1465472}{11025}\ln(v)^2 \right\} v^{12} + \dots - 722.42394673001478 \ln(v)^3 v^{18} + \dots \end{aligned} \approx \frac{2508888064}{3472875}$$

This result can be extended to the  $\ell > 2$  moments, using the methods developed in Ross, arXiv:1202.4750. The general pattern of logs is

$$|\mathcal{A}_\ell(\omega)|^2 \sim S(\omega) \sum_{n=1}^{\infty} \eta^{2n} L \left[ \beta_{2n}^{(\ell)} + \mathcal{O}(\eta^2 L) + \mathcal{O}(\eta^2 L)^2 + \mathcal{O}(\eta^2 L)^3 + \dots \right],$$

Sommerfeld

factor

$$S(\omega) = \frac{4\pi G_N m \omega}{1 - \exp(-4\pi G_N m \omega)}.$$

Fixes the series of logs

Maybe useful for the construction of phenomenological templates...

Other recent results in the radiation sector:

Radiation reaction at 3.5PN (1993-1995) (Galley+Leibovich, 2012). 4PN in progress (2011 Wang et al).

3PN Flux and 2.5PN waveform for spin-induced moments (Porto, Ross, Rothstein, 2010, 2012).

Hereditary terms in radiation reaction at 4PN (Foffa+Sturani, 2011) (Blanchet et al 2010)



# Dynamics and RG evolution of the mass mode

(WG, Ross, Rothstein, PRD 2013)

As we've seen, either a single compact object or a composite binary system is described by an EFT of the form

$$S = - \int d\tau(\lambda) M(\lambda) + \frac{1}{2} \int d\tau(\lambda) I^{ij}(\lambda) E_{ij}(\lambda) + \cdots$$

So far we have neglected the (slow) time dependence of the mass mode. The fact that mass is dynamical is a **requirement** of the **renormalizability** of the EFT

To track the time evolution of the mass mode we must employ **in/in boundary conditions**. Thus we compute the following matrix element

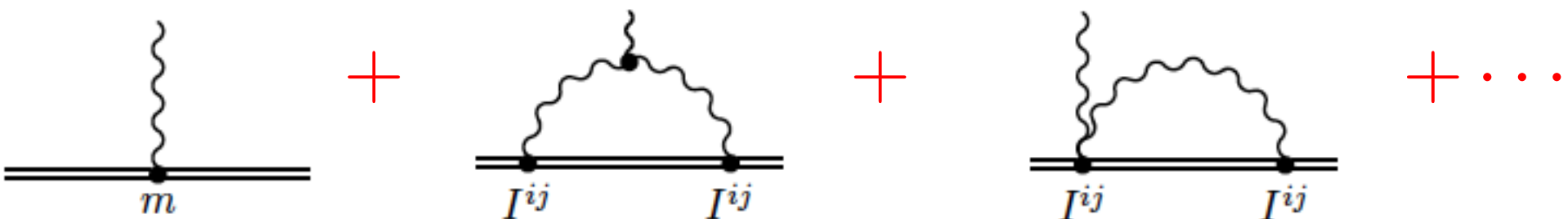
$$\langle in|T_{\mu\nu}(x)|in\rangle = - \frac{2}{\sqrt{g^+}} \frac{\delta\Gamma}{\delta\bar{g}_+^{\mu\nu}(x)} \Big|_{\bar{h}^+=\bar{h}^-=0}.$$

$$\partial_\mu \langle T^{\mu\nu} \rangle = 0$$

where the in/in effective action as a function of sources is

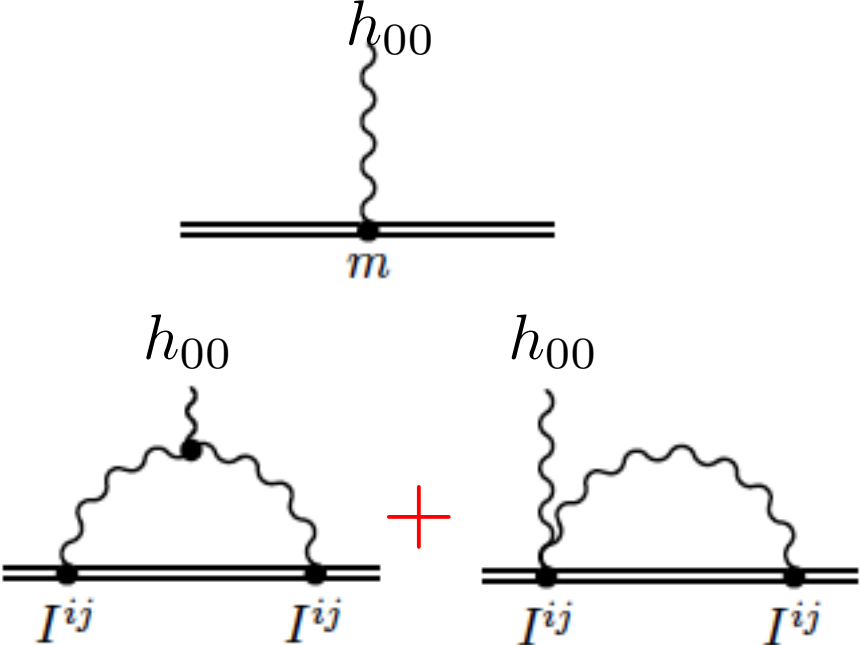
$$e^{i\Gamma[\bar{h}_+, \bar{h}_-, I, M]} = \int Dh^+(x) Dh^-(x) e^{iS[g^+, M, I] - iS[g^-, M, I]},$$

In terms of diagrams:

$$\langle T^{\mu\nu} \rangle =$$


where we drop terms that vanish in dimensional regularization.

Expanding in the  $\mathbf{k} \rightarrow 0$  limit (multipole expansion) one finds (in rest frame)



The diagrams show a mass  $m$  emitting a graviton  $h_{00}$  (top), and two diagrams of a quadrupole source  $I^{ij}$  emitting a graviton  $h_{00}$  (bottom left and right), separated by a red plus sign.

$$= \delta^3(\mathbf{x}) M(t)$$

$$= \delta^3(\mathbf{x}) \left[ \frac{G_N}{5} \int_{-\infty}^t dt' I_{ij}^{(5)}(t') I_{ij}^{(1)}(t') \right]$$

(net result for  $\langle T^{00} \rangle$  is **causal**, depending only on the past history of the sources)

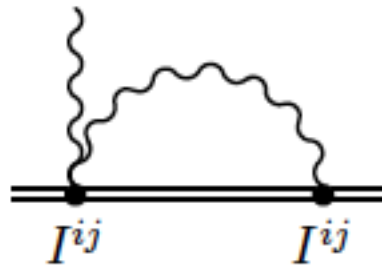
The time evolution of the mass mode is fixed by the Ward identity  $\partial_\mu \langle T^{\mu\nu} \rangle = 0$ .  
To leading order in the multipole exp. this is just

$$\frac{d}{dt} \langle T^{00}(x) \rangle = 0 \quad \longrightarrow \quad \dot{M}(t) = -\frac{G_N}{5} I_{ij}^{(5)}(t) I_{ij}^{(1)}(t)$$

Upon time averaging we reproduce the std. LO result  $\langle \dot{M} \rangle = -\frac{G_N}{5} \langle I_{ij}^{(3)} I_{ij}^{(3)} \rangle$

More generally,  $\partial_\mu \langle T^{\mu\nu} \rangle = 0$  determines how **all** the moments evolve in time due to radiative corrections (radiation reaction)

Note that the computing the diagram



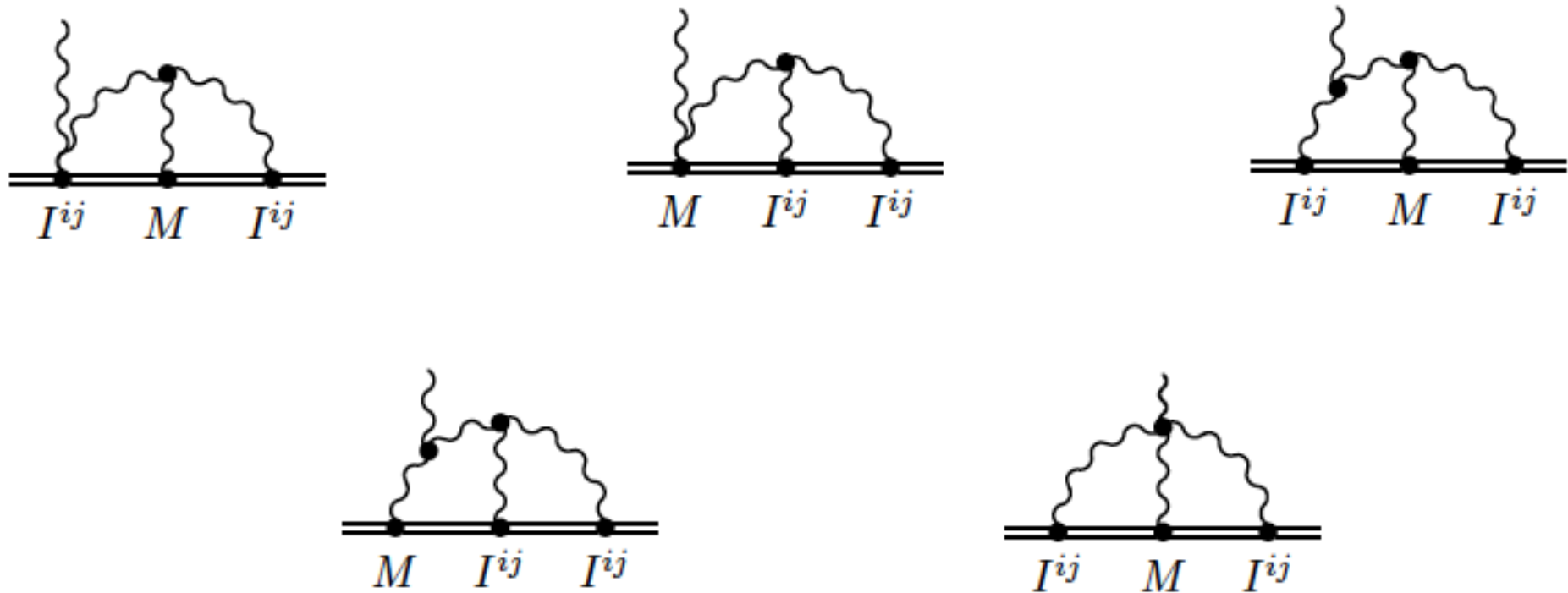
involves the Feynman integral

$$I = \int \frac{d^{d-1} \mathbf{q}}{(2\pi)^{d-1}} \frac{1}{\mathbf{q}^2 + \omega^2} = \frac{\Gamma(3/2 - d/2)}{(4\pi)^{(d-1)/2}} \omega^{d-3}$$

Although formally finite in dim. reg. as  $d \rightarrow 4$ , the integral is **linearly UV divergent** by power counting. A time dependent mass counterterm would be needed to renormalize this divergence.

This is why, in the EFT, the mass **must** become a dynamical variable, whose evolution is fixed by the condition the Ward id.  $\partial_\mu \langle T^{\mu\nu} \rangle = 0$

At the next order in the expansion, the UV divergences are **logarithmic**:

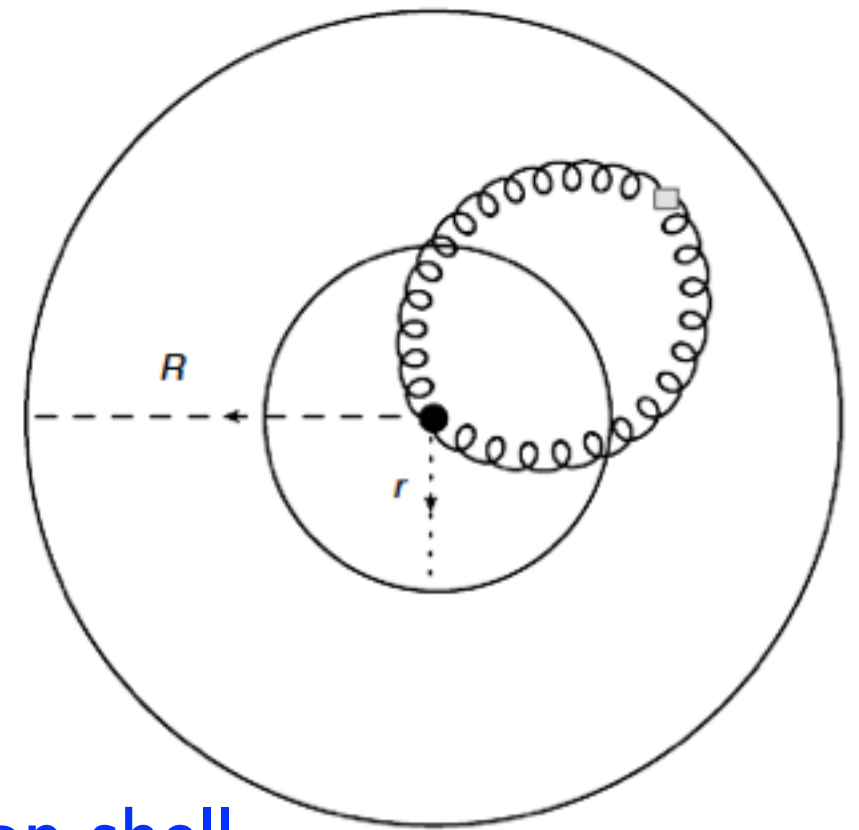


Leading to RG evolution of the mass mode (even under time reversal)

$$\mu \frac{d}{d\mu} M(t, \mu) = - \frac{2G^2 \bar{M}}{5} \left( 2I_{ij}^{(5)} I_{ij}^{(1)} - 2I_{ij}^{(4)} I_{ij}^{(2)} + I_{ij}^{(3)} I_{ij}^{(3)} \right) (t)$$

(on the RHS, to the order we work in, we treat the mass as a constant. We may as well take it to be the time averaged mass  $\bar{M} = \lim_{T \rightarrow \infty} \frac{1}{2T} \int_{-T}^T dt M(t)$  )

## Heuristic interpretation of RG running:



$M(t, \mu)$  is the **conservative mass** (not including on-shell radiation out to infinity). Varying the observation radius from  $\mu = 1/r$  to  $\mu = 1/R$  changes how much backscattered radiation is kept in the definition of  $M(t, \mu)$

To NLO  $M(t, \mu) =$  **Bondi mass**.  $M = \int d^3\mathbf{x} T^{00} =$  **ADM mass**

Can solve the coupled RGEs for  $M(\mu, t)$  ,  $I_{ij}(\mu, t)$  perturbatively:

$$\frac{\bar{M}(\mu)}{\bar{M}_0} = 1 - \frac{1}{2} \frac{\langle I_{ij}^{(3)} I_{ij}^{(3)} \rangle_0}{\bar{M}_0^2} r_s^2 \ln v + \frac{107}{420} \frac{\langle I_{ij}^{(4)} I_{ij}^{(4)} \rangle_0}{\bar{M}_0^2} r_s^4 \ln^2 v - \frac{11449}{132300} \frac{\langle I_{ij}^{(5)} I_{ij}^{(5)} \rangle_0}{\bar{M}_0^2} r_s^6 \ln^3 v + \dots ,$$

where we have run from  $\mu_0 \approx r_s = 2G_N M_o \rightarrow \mu = \omega$  to minimize “large logs”

Applications to high order log corrections to

**Graviton emission:**  $M \rightarrow M(\mu = \omega)$

$$\left| \frac{\mathcal{A}(\omega)}{\mathcal{A}_0(\omega)} \right|^2 = 1 + \pi r_s \omega - \frac{\pi}{2} \frac{\langle I_{ij}^{(3)} I_{ij}^{(3)} \rangle_0}{\bar{M}_0^2} r_s^3 \omega \ln v + \frac{107\pi}{420} \frac{\langle I_{ij}^{(4)} I_{ij}^{(4)} \rangle_0}{\bar{M}_0^2} r_s^5 \omega \ln^2 v + \dots$$

**“Lamb shift”:** Radiative correction to bound state energy:

$$E(\Omega) = -\frac{\mu^2}{M_0} \frac{448}{15} v^{10} \ln v + \dots ,$$

consistent with Blanchet et al 2010. (see also Galley, Leibovich, Ross; in progress).

# Summary and outlook

EFT methods provide a complete understanding of the dynamics of non-relativistic binaries. It has been used to obtain new results (particularly for spin) not yet achieved by traditional PN methods.

Some possible future directions:

On-shell amplitude methods? (see Neill+Rothstein, 2013).

RG from RW for  $\ell > 2$ ?

Other kinematic regimes?